HHS Public Access

Author manuscript

Eye Contact Lens. Author manuscript; available in PMC 2021 March 01.

Published in final edited form as:

Eye Contact Lens. 2020 March ; 46(Suppl 2): S84–S105. doi:10.1097/ICL.0000000000000684.

A Review of Imaging Biomarkers of the Ocular Surface

William W. Binotti, MD[1,2], **Betul Bayraktutar, MD**[1,2], **M. Cuneyt Ozmen, MD**[1,2], **Stephanie M. Cox, OD**[1,2], **Pedram Hamrah, MD**[1,2]

[1]Center for Translational Ocular Immunology, Department of Ophthalmology, Tufts Medical Center, Tufts University School of Medicine, Boston.

[2]Cornea Service, New England Eye Center, Tufts Medical Center, Tufts University School of Medicine, Boston.

Abstract

A biomarker is a “characteristic that is measured as an indicator of normal biological processes, pathogenic processes, or responses to an exposure or intervention, including therapeutic interventions.” Recently, calls for a biomarker for ocular surface diseases have increased, and advancements in imaging technologies have aided in allowing imaging biomarkers to serve as a potential solution for this need. This review focuses on the state of imaging biomarkers for ocular surface diseases, specifically non-invasive tear break-up time (NIBUT), tear meniscus measurement and corneal epithelial thickness with anterior segment optical coherence tomography (OCT), Meibomian gland morphology with infrared meibography and in vivo confocal microscopy (IVCM), ocular redness with grading scales, as well as cellular corneal immune cells and nerve assessment by IVCM. Extensive literature review was performed for analytical and clinical validation that currently exists for potential imaging biomarkers. Our summary suggests that the reported analytical and clinical validation state for potential imaging biomarkers is broad, with some having good to excellent intra- and inter-grader agreement to date. Examples of these include NIBUT for dry eye disease (DED), ocular redness grading scales, and detection of corneal immune cells by IVCM for grading of inflammation and monitoring. Further examples are nerve assessment by IVCM for monitoring severity of diabetes mellitus and neurotrophic keratitis, and corneal epithelial thickness with anterior segment OCT for diagnosis of early keratoconus. However, additional analytical validation for these biomarkers is required prior to clinical application as a biomarker.

Keywords

biomarker; imaging; ocular surface; NIBUT; IVCM; OCT

Corresponding author: Pedram Hamrah, MD, Tufts Medical Center, 800 Washington St., Boston, MA, 02111, United States, pedram.hamrah@tufts.edu; p_hamrah@yahoo,com.

Disclosures: PH is a consultant for Heidelberg Engineering

Supplemental Data. Non-invasive tear break-up time in a patient with dry eye disease with first and average tear break-up time of 1.7 and 4.7 seconds, respectively.

A biomarker has been defined by the United States National Institutes of Health (NIH) as a "characteristic that is measured as an indicator of normal biological processes, pathogenic processes or responses to an exposure or intervention, including therapeutic interventions", while a biomarker signature is a collection of measures that together serve as a biomarker.[1] Molecular-, epigenetic-, cellular-, and tear film protein-based biomarkers have previously been proposed.[2-4] Further, quantification of medical images has also been proposed for potential biomarker application.[5] The Quantitative Imaging Biomarkers Alliance (QIBA) has defined a quantitative imaging biomarker as "an objective characteristic derived from an in vivo image measured on a ratio or interval scale as indictors of normal biological processes, pathogenic processes, or a response to a therapeutic intervention".[5]

Biomarkers provide an objective, measurable method of evaluating a disease process. Some biomarkers aim to diagnose disease, which has an obvious translation to clinical care, but can also help researchers to more precisely identify the disease and thereby also identify the risk factors and early signs of the disease. Identification of the early signs of disease could lead to earlier treatments and better health outcomes for patients. Other biomarkers will allow drug developers to measure the effectiveness or safety of treatments. The most desirable biomarkers will be easily and rapidly quantifiable and cost-effective.

For assessment of ocular surface disease, many of our current metrics do not provide the specificity necessary to differentiate these conditions from each other, or allow proper differentiation of severity grades. For example, superficial punctate keratitis can be associated with blepharitis, ocular allergies, dry eye disease (DED), demodex, or contact lens complications, Therefore, biomarkers that have better specificity may allow patients to receive more targeted therapies. In addition, many patients have more than one ocular surface condition or several different or concurrent underlying etiologies. Therefore, clinical trials treating one condition and using only subjective symptom questionnaires may underestimate the effectiveness of treatments because the trial drug is only targeting one of the conditions or one underlying factor that results in patient symptoms. Thus, objective biomarker are needed for ocular surface disease that could allow for better diagnosics, and for monitoring effectiveness of therapeutic interventions.

Any proposed biomarker should thus be evaluated for its analytical and clinical validation (Tables 1 and 2).[1,6] Analytical validation can be thought of as an evaluation of the imaging device and/or classification scheme developed from image parameters and requires demonstration of accuracy, precision, and feasibility of the biomarker. Clinical validation can be thought of as the evaluation of the imaging parameter's ability to work as a biomarker in the proposed population and/or its association with clinical endpoints. Types of biomarkers include susceptibility/risk biomarkers, diagnostic biomarkers, monitoring biomarkers, prognostic biomarkers, predictive biomarkers, pharmacodynamics/response biomarkers, and safety biomarkers.[1] The statistics associated with the validation of biomarkers is discussed in more detail within the methods section. In each specific section below, the analytical and clinical validation status of potential biomarkers have been defined separately and their respective current states has been summarized.

Methods

The potential imaging biomarkers selected for inclusion in this review were based on imaging parameters that could be obtained with devices currently available to clinicians and not experimental devices or prototypes. Electronic searches of PubMed were used to analyze the literature for each potential biomarker. Search terms included “tear break up time AND repeatability,” “tear break up time AND reliability,” “tear break up time AND sensitivity,” “tear break up time AND specificity,” “tear break up time AND treatment,” “tear break up time AND correlation,” “tear break up time AND dry eye disease,” “non-invasive tear break up time,” for NITBUT; “tear meniscus height,” “tear meniscus area,” for tear meniscus measurement; “meibography,” “meibomian gland drop out,” “anterior segment optic coherence tomography,” for meibomian gland morphology; “in vivo confocal microscopy,” and its different combinations with; “corneal nerve,” “corneal density,” “nerve morphology,” “nerve tortuosity,” “nerve beading,” “nerve reflectivity,” “nerve thickness,” “neuroma,” “neuropathic corneal pain,” “diabetes mellitus,” “systemic disease,” “sensitivity,” “specificity,” “keratitis,” “acanthamoeba,” “fungal keratitis,” “demodex,” for corneal nerve alterations and qualitative biomarkers; “epithelial corneal thickness,” “keratoconus AND anterior segment oct,” “limbal stem cell deficiency AND anterior segment oct,” “subclinical keratoconus AND anterior segment oct,” “dry eye disease AND anterior segment oct,” for corneal thickness and epithelial thickness; “ocular redness,” “ocular redness grading,” “ocular redness scale,” “conjunctival hyperemia,” “bulbar redness,” “bulbar hyperemia,” “dendritic cell,” “dendritiform cell, “palpebral inflammation,” “in vivo confocal microscopy” for ocular surface inflammation. The results of this search were supplemented by abstracts from the authors in order to provide the most updated data available for each potential biomarker. Manuscripts/abstracts were examined for the inclusion of one aspect of analytical or clinical validation discussed below. After completion of the manuscripts/abstracts, the results were used to evaluate each potential biomarker’s analytical and clinical validation.

Analytical validation should include verification of the accuracy of the biomarker. For imaging biomarkers, this verification should prove that the structure within an image is being named the correct anatomical structure. Quantitatively, analytical validation includes repeatability and reproducibility. Repeatability and reproducibility address the variability that is possible between visits in the same subject due to differences in examiner, environment, etc. These are often quantified using intraclass correlation coefficients (ICC), kappa values (only for categorical data), coefficients of variability/variation (CoV), and the repeatability coefficient. If ICC is used, poor, moderate, good, and excellent agreement is defined by values of less than 0.50, 0.50 to 0.75. 0.76 to 0.90, and greater than 0.90, respectively. If Kappa is used, no, minimal, weak, moderate, strong, and almost perfect agreement is defined by values of less than 0.20, 0.21 to 0.39, 0.40 to 0.59, 0.60 to 0.79, 0.80 to 0.90, and greater than 0.90, respectively. Weighted kappa can also be used, which is typically larger than unweighted kappa values, because it takes into consideration the amount of disagreement. For example, grades of 1 and 2 for the same image are not considered the same amount of disagreement as grades of 1 and 4. This extent of disagreement is taken into consideration in a weighted kappa value but not an unweighted

kappa. CoV is calculated by dividing the standard deviation by the mean. This ratio, which is often represented as a percentage, can be any positive number including zero. If necessary, CoV values reported in manuscripts were converted to percentage by the authors. The repeatability coefficient is derived from the within subject standard deviation. Ranges defining poor, moderate, good, and excellent repeatability do not exist for CoV and repeatability coefficient values; however, they can be compared to each other within the same biomarker provided the measures are absolute instead of relative.

Statistics required for clinical validation is dependent on the biomarker type being tested. It should be noted that a biomarker validated for one purpose does not necessarily mean that it can be used for another purpose. For example, a biomarker may be ideal for use as a diagnostic biomarker, but not as a monitoring biomarker. Diagnostic biomarkers typically are validated by measures of sensitivity, specificity, and/or receiver operating curves. Manuscripts reporting significant differences between groups are valuable in identifying imaging parameters that could be pursued as potential diagnostic biomarkers. However, the diagnostic validation step should consider if more than one disease/condition is capable of causing a reduction/increase in a potential biomarker compared to a control group. If this is true, the potential biomarker may not be useful in diagnosis due to low specificity. Monitoring biomarkers could be validated by correlating changes in the biomarker with changes in the status of the disease. Prognostic, predictive, safety, and susceptibility/risk biomarkers can be validated with survival analyses and/or odds ratios. Alternatively, these biomarker types may be able to be validated by comparing the response of those who were administered a therapy to those who were not when the two groups are further divided by presence/absence of the biomarker. Pharmacodynamic biomarkers may be validated by comparing the change in the biomarker in a group of patients who were given a control/standard treatment to that of a test treatment/environmental agent.

This review aims to provide an overview of the state of validation of current and potential imaging biomarkers for ocular surface diseases. The text provides a descriptive and interpreted analysis for each potential biomarker. Supportive quantitative data is provided in Tables 3 and 4.

Tear Film Assessment

Non-Invasive Tear Break Up Time (NIBUT)

The tear film plays a key role in maintaining ocular surface health and quality vision. The tear break-up time (TBUT) reflects the quality and stability of the tear film and is reduced in patients with an evaporative component of DED, compared to normal subjects.[7-9] Most commonly, reduction in TBUT is associated with a compromised tear lipid layer; however, mucin and tear dynamics have also been cited as contributors to TBUT changes.[9,10] Traditionally, assessment of TBUT is performed after instillation of fluorescein dye, which enables visualization of the tear film; however, the amount and concentration of fluorescein, as well as timing of assessment and humidity can cause variability and lack of adequate reproducibility.[11-15]

The NIBUT attempts to eliminate the variability of TBUT caused by fluorescein dyes through imaging. It utilizes disruptions in a regularly patterned image (grid or concentric circles typically), projected onto the tear film to identify areas of tear film disruption (Fig. 1). The measurement of NIBUT initially required a subjective measurement by an examiner and results show a longer break-up time for a subject when compared to their fluorescein TBUT.[16] More recently, the development of new devices with automated softwares for NIBUT quantification through detection and mapping of tear film break-up location over time, has attempted to eliminate inter-grader variability observed with subjective examiner assessment.[17,18] Initial studies with these softwares reported shorter break-up times compared to TBUT;[17,19] however, longer break-up times were also reported afterwards.[20] Despite different comparative results with TBUT, NIBUT with a cut off value less than or equal to 10 seconds has now been identified by the Dry Eye Workshop II (DEWS II) as an indicator for DED diagnosis with 82-84% sensitivity and 76-94% specificity.[21]

Analytical Validation—Accuracy of NIBUT was determined by comparing NIBUT values to those obtained via the gold standard TBUT. Significant correlations between these values have been reported.[18,22,23] However, while some studies have reported that TBUT is longer than the NIBUT,[18,20,22] others have reported the opposite.[23,24] The reason for the varying reports may be due to different subject cohorts (DED vs. control subjects, age, etc.).

The cut-off value for abnormal NIBUT can be assumed to be less than 10 seconds. There was less variability when the determination of NIBUT was made by software instead of the clinician.[25] As such, the Reported ICC values suggest good to excellent repeatability for automated NIBUT; however, there was a large CoV range suggesting unknown amount of variability, which means NITBUT does not exhibit consistent repeatability, and a wide range of repeatability has been reported by different groups (Table 3).[18,23,25-27] It was also noted that the variability of the NIBUT was greater at greater values of TBUT.[24] Overall, ICC values suggest good reproducibility CoV ranged from 15.4% to 21.85% (Table 3).[18,26] However, low ICC values suggest there was little agreement between two devices that provide NIBUT,[28] suggesting that measures from different devices should be compared with caution.

Clinical Validation—The sensitivity and specificity of NIBUT provides an assessment of its ability to act as a diagnostic biomarker. When the DEWS II cut-off of 10 seconds is used to differentiate DED from controls (Fig. 1), NIBUT provides a sensitivity of at least 80.0% and a specificity of at least 86.0.[29-31] Other cut-off values have been proposed, but the evidence does not support a clinically significant improvement in sensitivity and specificity compared to the 10 second cut-off. [23,19,32].[18] In addition, NIBUT has been used to show improvements (increase) with treatment, suggesting that it could be used as a monitoring biomarker,[33,34] albeit inconsistently.[35] Thus, additional data is needed to support the utilization of NIBUT as a monitoring biomarker, a process that can be accelerated by encouraging more studies to employ NIBUT methods, rather than the currently prevalent fluorescein TBUT approach.

In summary, the validation of the NIBUT as a diagnostic biomarker for DED has been investigated, and its' good sensitivity and specificity values suggest that it is appropriate for

utilization. Further, NIBUT shows good repeatability and reproducibility as a diagnostic biomarker. However, the larger variability it suffers is derived from the larger variation at higher values. This is common in other measures as well and should be taken into account during biomarker validation and when applied in a clinical setting. Further, these variations could also be reflecting disease processes. Evidence also suggests that NIBUT has potential as a monitoring or predictive biomarker in DED; however, further work is necessary to support its utilization in this regard. Current literature to support the potential of NIBUT to be used as a prognostic, safety, susceptibility/risk, or pharmacodynamic biomarker does not currently exist.

Tear Meniscus Measurement by Anterior Segment Optical Coherence Tomography (OCT)

The lower eyelid tear meniscus can be measured for tear meniscus height (TMH) and/or tear meniscus area (TMA),[36] which have been found to be reduced in aqueous-deficient DED.[37] As such the DEWS II report suggested that TMH be used for diagnosis of aqueous-deficient DED.[36,38-40] The utilization of techniques with infrared light and anterior segment OCT, using low coherence light, allows TMH and TMA to be measured without reflex tearing, which has improved its accuracy.[41-44] The main anterior segment OCTs used to date are time-domain (TD-OCT) and spectral-domain OCTs (SD-OCT),[45] with the latter performing scans at a much faster rate. Spectral-domain OCTs have improved resolution and a significantly higher acquisition speed, resulting in improved image quality, and minimized motion artefacts compared to TD-OCTs.[46] Moreover, a different OCT modality called swept-source (SS-OCT) has more recently become available.[45] One of the advantages of SS-OCT imaging over SD-OCT is the faster scanning speed, which allows for denser scan patterns and larger scan areas compared with SD-OCT scans for a given acquisition time. Additional advantages of SS-OCT technology are its use of a longer wavelength and its reduced sensitivity roll-off, resulting in better detection of signals from the deeper layers.[47]

Analytical Validation—Reported mean TMH values in samples of normal subjects are varied, but are less than 0.354 mm, regardless of type of anterior segment OCT (Table 3). The measures gained via anterior segment TD-OCT and SD-OCT are typically lower[39] and SS-OCT is higher,[48] compared to those obtained via slit-lamp. Therefore, normative database and cut-off values for each device are recommended and different measurements between OCTs and slit-lamp are explained by nature of imaging technique and image processing procedures.[39] The range of inter-grader ICC values is smaller for anterior segment OCT and are considered good to excellent.[15,39,48-50] When compared to time domain OCT, spectral domain OCT has shown better intra- and inter-grader agreement in most studies based on reported CoV values and narrower 95% confidence intervals. In addition, the ICC values suggest excellent repeatability.[51] Further, swept-source OCT has shown excellent repeatability as well; however, the CoV values for intra- and inter-grader repeatability are comparable or better to spectral domain OCT (Table 3).[39]

The mean normal TMA range has been reported with high variability based on the anterior segment OCT methods used (Table 3).[37,40,42,48,52,53] TMA measurements tend to be larger with time domain OCT as compared to spectral domain OCTs. Overall, based on the current literature, spectral domain OCTs provide superior intra- and inter-grader repeatability

compared to time domain and swept-source OCTs, even though the intra- and inter-grader ICCs with swept source OCTs were moderate-to-high (Table 3).

Clinical Validation—TMH as a diagnostic biomarker for DED using TD AS-OCT has shown a 67.0% sensitivity and 81.0% specificity (Table 3). In comparison, SD AS-OCT demonstrates 80.5% sensitivity and 89.3% specificity for TMH and 86.1% sensitivity and 85.3% specificity for TMA. The diagnostic ability is best for Sjögren's aqueous-deficient DED and is moderately acceptable (i.e., just greater than 65%) for non-Sjögren's aqueous-deficient DED. In comparison, the diagnostic ability for evaporative DED is less than 50%.[54]

Like TMH, TMA has better sensitivity with spectral domain compared to swept-source anterior segment OCT, but worse specificity (Table 4). TMA has shown better diagnostic ability than TMH in evaporative DED, non-Sjögren's aqueous-deficient DED, and Sjögren's aqueous-deficient DED.[54] However, the accuracy is above 70% only in non-Sjögren's aqueous-deficiency and Sjögren's aqueous-deficiency DED. Interestingly, El-Fayoumi et al. have shown a decreased TMH and TMA in rheumatoid arthritis patients, compared to healthy controls, despite the absence of clinical diagnosis of DED.[55] Because TMH and TMA changes were present prior to a diagnosis of DED, they may be useful as suspectibility/risk biomarkers; however, extensive additional work would be needed to validate TMH and TMA for these purposes.

The TMH and TMA on all OCT devices have been used as a monitoring biomarker to assess changes in tear meniscus following DED treatment[56-58] or to assess the effect of contact lens wear.[59] Increased tear meniscus measurements after installation of artificial tears, diquafasol sodium and rebamipide were reported in DED.[56,60] Furthermore, decreased tear meniscus height with contact lens wear and improvement after installation 3% diquafosol solution has also been reported.[59]

Standardization of TMH and TMA measurements and potentially automated methodologies would be helpful in ensuring additional analytical validation. Furthermore, when using TMH or TMA in a clinical trial setting, some limitations should be considered when interpreting the outcomes. These include the presence of conjunctivochalasis, time-from-blink, and the prevailing environmental conditions, all of which may cause additional variability of both TMH and TMA measures.[21]

In summary, TMH and TMA have acceptable diagnostic ability in DED, especially in aqueous deficiency DED. Additionally, these parameters can be helpful in early diagnosis of DED in systemic conditions. However, normative databases, cut-off values and standardized acquisition methods should be described for each device. Altogether, the use of TMH and TMA as diagnostic and monitoring biomarkers appears promising.

Assessment of Meibomian Gland Morphology

Meibomian glands (MG) are modified sebaceous glands situated in the tarsal plate of the upper and lower eyelids and produce meibum, which is essential to stabilize the tear film and decrease evaporation. MG dysfunction (MGD) was defined by The International Workshop

on Meibomian Gland Dysfunction (MGD Workshop) as “chronic, diffuse abnormality of meibomian glands that is commonly characterized by terminal duct obstruction or qualitative or quantitative changes in glandular secretion”.[61] MGD can result in more rapid tear film evaporation and may lead to DED. Therefore, evaluation of MG function and/or morphology is required for the diagnosis of MGD.[9] To date, MG morphology has been assessed anatomically by infrared meibography and at a cellular level by *in vivo* confocal microscopy (IVCM).

IVCM parameters that could be used as biomarkers, include MG orifice width (Fig. 2a), MG acinus descriptors, such as short diameter, long diameter, and density.[62] However, the images provided in publications identified by authors as presumed MG acini vary widely in morphology.[62-78] In fact, a recent study provided histological evidence that image appearance refined in some studies as presumed MG acini were actually rete ridges of the conjunctiva.[79] This highlights the importance of accuracy in analytical validation and the lack of its current availability regarding MG acini and IVCM. Given the lack of consensus regarding MG acini morphology by IVCM, parameters related to the MG acini will not be discussed in this review.

Infrared Meibography

MG dropout is defined as areas showing a loss of acinar tissue as identified by meibography.[61] An example of MG dropout can be seen in Fig. 3. Even though evaluation of MGs by transillumination has been described decades ago, MG dropout has been more widely used since the introduction of non-contact infrared meibography, which has a shorter acquisition time, higher image quality, and less patient discomfort.[80] Several devices have been developed that can acquire the images necessary for the assessment of MG dropout, and several grading scales for MG dropout have since been presented.[80-82] Two grading scales, the Gestalt grading scale and Meiboscale, were recommended by the MGD Workshop and will be evaluated in this review. In the Gestalt grading scale, a partial gland was defined as “one that is incomplete and present in clumps or clusters.” Each lid is graded based on the percent of partial glands, such that Grade 1 is no partial glands, Grade 2 is less than 25% partial glands, Grade 3 is 25-75% partial glands, and Grade 4 is greater than 75% partial glands. In the Meiboscale, each lid is graded based on percent dropout as follows: Grade 0: no loss of meibomian glands, Grade 1: area loss less or equal to 25%, Grade 2: area loss less than or equal to 50%, Grade 3: area loss less than or equal to 75%, and Grade 4: area loss less than or equal to 100%.[80] More recently, continuous grading scales based on a semi-automated software have been developed. This semi-automated software is used to outline the total MG area and the part of the area that has MG dropout. The dropout area is then divided by the total area to give a percent of dropout that ranges between 0% and 100%.[83] One of the obvious advantages of the continuous scale is that small changes can be reflected with the continuous grading scale that may not be shown in the categorical grading scales. For example, a subject with 10% drop out who progresses to 20% drop out would be in the same meiboscore grading, but this change would be reflected in the continuous grading scale.

Additional parameters associated with meibography include MG bend, MG thickness,[84] MG distortion, tortuosity, hooking, shortening, thickening, thinning, overlapping, and ghosting. One study clearly defined these parameters and assessed the intra- and inter-grader agreement of these parameters and reported low values of agreement, suggesting that they may not be ideal biomarkers.[85] This lack of agreement suggests little promise for MG bend, MG thickness, MG distortion, tortuosity, hooking, shortening, thickening, thinning, overlapping, and ghosting to become biomarkers. Given the lack of additional publications assessing these parameters, we will not further assess these parameters here.

Analytical Validation—The accuracy of infrared meibography is supported by a histological study that included analysis of light transmission through the MG.[86] This report showed that the meibum within MG acini cells scattered infrared light and caused the MG to appear white in the infrared meibography images.[86] The authors also noted that the extent of light scattering appears to be greatest in areas that contain small lipid droplets, which were identified using neutral lipid fluorescent staining, as opposed to areas with coalesced lipid droplets or areas without lipid droplets.[86] Although it should be noted that other abnormalities, such as concretions, can also reflect light in a similar way to MGs and can therefore be confused with them.[87] The extent of MG dropout is age dependent even in non-DED patients.[88] Therefore, normative values are different for various ages. The MGD Workshop proposed the following cut-off values: patients 20 years of age or less should have no dropout and patients over 20 years of age may have less than or equal to 25% dropout.[83]

Repeatability of MG dropout is dependent on the repeatability of 1) image acquisition and 2) the grading scale. Image acquisition can be affected by the positioning of the lid during eversion and the patient's direction of gaze, both of which can change even within a single session.[89] It can also be affected by the ability of the eyelid to evert, which is inconsistent across subjects.[85] The intra-grader weighted kappa values for the Gestalt grading show a large range from no agreement to almost perfect agreement (Table 4). [81]In addition, less agreement was present in patients with greater MG loss [weighted kappa = 0.79 (95% CI: 0.69-0.88)] compared to those with less/no MG loss [weighted kappa = 0.82 (95% CI: 0.73-0.91)].[81] For the meiboscale, the reported intra-grader agreement ranged from weak to strong when weighted kappas were evaluated and minimal when unweighted kappas were considered.In one study that compared these subjective grading scales, the meiboscale showed better intra-grader agreement, compared to Gestalt grading.[82] When a continuous grading scale was used, the intra-grader ICC values showed moderate agreement.[85] The ICC was higher (although not statistically significant) when areas of indistinct MG appearance were classified as drop out, compared to when they were not, suggesting that such directives, training, or computer automation that reduces grader subjectivity, may assist in improving intra-grader agreement.[85]

Reproducibility studies have shown that meibography devices can provide varying images due to variability in amount of lid everted and image quality, causing differences in MG drop out gradings[90] and quantitative image analysis.[91] This suggests that if MG dropout is used as a biomarker to monitor disease progression, the same device should be used consistently throughout all visits. In addition, the upper and lower eyelids should be graded separately based on evidence that there is a significant difference in MG area/total analysis area

between upper and lower lids, especially in eyelids with lower level of dropout.[84,92] The weighted and unweighted inter-grader kappa statistics for the Gestalt grading and the meiboscale showed large agreement ranges for upper and lower eyelids.[81,82] In general, inter-grader agreement was better for the upper eyelids compared to the lower eyelids.[93] However, for the continuous grading scale, the inter-grader ICCs show moderate to good agreement[85,93] and there was approximately equal amount of agreement for the upper and lower eyelids.[93]

While the accuracy for infrared meibography has been addressed, the repeatability and reproducibility is inconsistent. This inconsistency, especially with the categorical grading scales, suggests that a more standardized protocol should be used across multiple studies, in order to improve the consistency of image acquisition and grading, and thereby the analytical validation. In addition, the utilization of a continuous grading system appears to be better than a categorical system. Incorporation of the continuous grading scale into a clinical setting may necessitate the use of artificial intelligence in order to address problems of feasibility.[61,82]

In summary, MG dropout may be affected by image acquisition methods and grading scales. To minimize image acquisition related problems, same devices should be used during monitorization. Methods to standardize eyelid eversion should be developed and upper/lower eyelids should be graded and compared separately. To decrease grading scores related problems, continuous grading systems seems to be promising and may be implemented into clinical practice. MG dropout may be a good candidate as a diagnostic biomarker; however, its use as a biomarker for monitoring treatment response needs to be established further.

Clinical Validation—MG dropout was a significant discriminator between DED and control subjects when they were diagnosed based on OSDI score.[84] This parameter has also proven to be useful in discriminating between aqueous-deficient and evaporative DED, suggesting that MG dropout may be a good diagnostic biomarker.[94] A proposed meiboscore cut-off value of three for diagnosis of MGD provided 49.3% sensitivity and 64.5% specificity.[95] However, in a recent study based on a different subjective grading scale,[81] the sensitivity and specificity of a cut-off value of 0.75 were reported with 87.9% and 100%, respectively. Moreover, MG dropout did not predict effectiveness of liposomal spray, latent heat goggles, and warm compresses,[96] suggesting that it is not a good predictive biomarker. In summary, both upper and lower eyelid drop out has been correlated with lipid layer thickness, NIBUT, OSDI, and age, suggesting it may be useful as a monitoring and/or pharmacodynamic biomarker. Currently, literature to suggest that MG drop out could be used as a prognostic, safety, or susceptibility/risk biomarker is not available.

Ocular Surface Inflammation

Conjunctival Redness

Bulbar conjunctival hyperemia is caused by vasodilation, increased blood flow and capillary permeability associated with ocular surface inflammation, and is one of the most common clinical signs perceived by the patient that can correlate to inflammation of the ocular surface and is often the main cause for seeking medical care.[97-99] However, inflammation

can be subclinical, such as in DED, and may not be detected by slit-lamp examination or perceived in early disease.[74] Previously, ocular redness assessment relied on ordinal scales to classify the severity ranging in a 4 or 5 category scale from normal or trace to severe (Fig. 4).[100,101] When these scales are applied to photographs, they become part of the potential biomarker, and thus, should be validated like other imaging biomarkers.

Analytical Validation—The analytical validation of the ocular redness as a biomarker is dependent on consistency of image capture (illumination, white balance, magnification or image color resolution) and validation of the grading scales. The most common ocular redness scales, such as Efron, CCLRU, Vistakon and Annunziato have shown no statistically significant bias between the test/retest grading within observers (i.e. intra-grader agreement)[100,102].The inter-grader coefficient of repeatability ranges from 0.49 to 0.80 grading units,[102,104,105] which suggest that two graders should grade the same image within approximately 1.5 steps of another grader. Given that the scales are only typically 4 or 5 steps, there is a significant inter-grader variability with these scales. However, such scales have a high subjectivity and are prone to: 1) variations of photographic devices, such as illumination, white balance, magnification or image color resolution, 2) inter-grader variability and bias, such as judgment influence bias based on previous grading, and 3) inherit limitations of the grading scales, which have low discriminatory degree of severity (4 or 5 stages) to detect small incremental changes that occur in OR and show inconsistency with regards to the proportional severity between the representative image within the same scale or between different scales.[102,105,106] As such, the same grade in one scale might be perceived differently in another scale, not allowing comparison between studies with different scales.

One attempt to address these issues was with the Validated Bulbar Redness (VBR) grading scales that are based on the psychophysical attributes of graders during the validation process, by choosing representative images from a continuous grading scale ranging from 0-100 with equal steps of severity.[107] This scale showed an excellent intra-grader repeatability and inter-grader reproducibility for clinical assessment of ocular redness and has been validated against previous scales (Table 4).[107] Further, the Ocular Redness Index (ORI) performs a white-balance that corrects for lighting and color imbalance of slit-lamp photographs to provide an automated redness quantification of the selected region of interest.[108] This method has not only shown a high interobserver agreement and a strong correlation with subjective ocular redness and VBR scales, but also no significant disagreement or bias between graders. Amparo et al. compared the automated ORI to validated bulbar redness grading scales. This study showed that although both systems were capable to identify significant changes in mean redness scores, there was a significant level of disagreement in validated bulbar redness scores among experienced clinicians.[103]

In summary, ocular redness grading scores have some limitations caused by image capturing, intergrader differences, and intragrader bias, based on previously assessed images (use of previous image as a reference), and low discriminatory degrees of severity. Automated systems may be useful to overcome these limitations.

Clinical Validation—Ocular redness provides a metric to record and monitor the natural course of ocular surface diseases. The subjective ocular redness scales have been the most commonly used and in a wide range of diseases, specifically to compare the adverse effects of different contact lens materials and solutions on the ocular surface,[102,109,110] as well as topical and surgical interventions for glaucoma,[111,112]suggesting that it could be used as a safety biomarker. These scales have also been used to assess the effects of topical anti-allergic drops[113-115] and anti-inflammatory drops in various ocular surface diseases,[116-119] suggesting that it could be used as a monitoring biomarker. Recently, the ORI has been used to report conjunctival hyperemia changes in patients undergoing pterygium surgery, showing a potential to discriminate statistically significant ocular redness changes (26%) that were imperceptible to clinicians,[103] thus supporting the utilization of such a system.

Due to the numerous conditions that present with ocular redness, its utilization as a diagnostic biomarker seems improbable. In addition, evidence does not support the notion that ocular redness could be used as a predictive, susceptibility/risk, or pharmacodynamic biomarker. However, evidence does exist that ocular redness could be used as monitoring and safety biomarkers. Although the use of ocular redness grading systems is well established in ophthalmology and currently used for clinical trials, the more recent ORI measures have not reached the same level of evidence for clinical trials and require randomized and multi-center studies for further clinical validation. However, the ability of the ORI to detect smaller changes in ocular redness is promising and further work could elicit the utilization of ocular redness as a biomarker. Nevertheless, the main limitation that remains is the inability of this parameter to detect subclinical inflammation.

Cellular Quantification by *In Vivo* Confocal Microscopy

Although the normal cornea was thought to be immunologically privileged due to its lack of immune cells during homeostasis, the presence of resident immature dendritic cells and other resident corneal leukocytes has been clearly demonstrated by many independent groups.[120-127] These resident leukocytes can be visualized at the basal epithelial layer by IVCM as dendritiform cells (DCs; Fig. 5a). During inflammation, DC density increases along with elongation of their dendrites, which is associated with DC maturation (Fig. 5b-c).[121,122,128] Therefore, not only DC density, but also DC size, and DC field are potential parameters to evaluate the inflammatory state of the cornea.

Analytical Validation—IVCM is a non-invasive tool capable of microscopically imaging DCs of the ocular surface with a direct correlation to immunohistochemical DC observations.[123,129] This supports the accuracy of IVCM in imaging DCs. Further, it has been shown that the structural analyses of three representative central corneal images are comparable to wide-field composite images of the subbasal layer in chronic inflammatory conditions.[130] In healthy individuals, DCs are located mostly in the subbasal epithelial layer with a reported average density 9-64 cells/mm^2 in the central cornea and 0-208 cells/mm^2 in the peripheral cornea.[75,131-139] The assessment of the average DC density has shown intra-grader repeatability with low CoV (4.4-11.9%) and excellent inter-grader reproducibility (Table 4).[74,134,135,137-139] However, increased variability was reported with increased DC densities.[140] A more recent study reported promising results for detection of DCs through

artificial intelligence. Initial sensitivity rates for DC detection and DC segmentation were reported as 85% and 60%, respectively.[141]

Clinical Validation—An increase in mean corneal DC density above normal values is considered an indicator for active immune response or inflammation in the cornea.[137,142] Increase in DC density has been reported in DED,[64,136,144-147] allergic keratoconjunctivitis,[148] infectious keratitis,[149,150] herpetic keratitis,[138] contact lens wear,[151] post-LASIK cases,[151] glaucoma medication use,[152-155] thyroid ophthalmopathy,[156] and systemic diseases.[157-161] It has been demonstrated that aqueous-deficient DED exhibits higher DC density compared to evaporative DED and that aqueous-deficient DED related to systemic immune diseases showed higher DC density compared to non-immune conditions.[136] In addition to DC density, DC size, and DC field were significantly increased in Sjögren's DED compared to non-Sjögren's DED.[136]

It has been shown that there was a strong significant correlation of DC density with symptoms (OSDI) (r=0.37), Schirmer's test (r= −0.47), TBUT (r= −0.61 to −0.25), corneal fluorescein staining (r= 0.48 to 0.53) and levels of various inflammatory tear cytokines (r= 0.31 to 0.55), which demonstrates its strong correlation with inflammation in DED patients.[140,144,150,162-165] In a prospective, cross-sectional study it was further reported that at peripheral corneal quadrants DC density had different correlations with TBUT (r= −0.49 to −0.28), corneal fluorescein staining (r= 0.33 to 0.40), and conjunctival staining (r= 0.24 to 0.35).[166] Therefore, In addition to DC density, the morphology and distribution of DCs with their aforementioned correlations may further help establishing this parameter as a diagnostic biomarker for the DED subgroups.

From the perspective of a predictive biomarker, it has been shown that treatment response, based on change in OSDI and DC density, to topical steroids was correlated with baseline DC density and patients with increased DC density at baseline yielded a pronounced decrease in DC density with topical steroid treatment. Villani et al reported in a prospective, open label, masked study, that baseline DC density was correlated with OSDI and DC density changes in DED patients treated with topical steroid.[144] Moreover, a recent, prospective, randomized, placebo controlled, clinical trial confirmed that a DED population enriched with increased DCs for inclusion, yielded a pronounced decrease in DC density and significant improvement in signs and symptoms with topical steroid treatment.[163,167]

Furthermore, DC density has also been shown a reliable tool in quantitative detection and monitoring of many ocular inflammatory diseases.[149,150,168-173] In conditions such as DED, bacterial keratitis and post-LASIK ectasia correlation between proinflammatory cytokines (e.g. for bacterial keratitis IL-1β, IL-6, and IL-8, r= 0.40, r= 0.55, and r=0.31, respectively; $p<0.002$) and DC density was defined.[150,174,175] In the context of recurrent herpetic keratitis, DC density by IVCM has been shown to be a powerful tool to detect early signs of intracorneal inflammatory activity, which allows early detection and treatment, leading to improved prognosis.[170,176] Therefore, in inflammatory conditions, DC density may be helpful as a monitoring and pharmacodynamics biomarker.

Assessment of DC density through IVCM has been reported with extensive analytical validation, showing excellent repeatability and reproducibility. Recent studies on DED report the presence of subclinical immune cells in the ocular surface as a possible explanation for the symptom-sign disparity in DED and symptom refractory despite improvement of current clinical tests.[74,75,144] These results suggest that IVCM can detect early subclinical inflammation, allow treatment stratification, and measure therapeutic response according to baseline DC density as a predictive and/or response biomarker. Lastly, the DC density measurement has shown growing evidence as a diagnostic biomarker for the presence of inflammation in the ocular surface and is valuable both as a monitoring and pharmacodynamics biomarker to be used in clinical trials for various ocular surface diseases. Thus, it may serve as a useful monitoring biomarker for inflammatory conditions, such as in DED,[143,177] ocular allergies,[148] and contact lens wear, and pharmacodynamics biomarker for treatment response of those conditions.[151]

Palpebral Inflammation—Laser IVCM is a non-invasive technique that has been utilized to assess the immune cell density in IVCM images at epithelial and stromal levels (Fig. 2b).[178] Immune cell density is typically completed using semi-automated software that allows the cells to be marked and counted. That count is then typically standardized to cells per millimeter square.

Analytical Validation—Normative values for immune cell density have been reported as 123.3-123.7 (standard error = 17.2-19.2) cells/mm^2 for the epithelium and 36.7-38.8 (standard error = 9.5-10.2) cells/mm^2 for the stroma (Table 4).[74,75] The intra-grader repeatability showed excellent agreement for the epithelial immune cell (EIC) density and for the stromal immune cell (SIC) density (Table 4).[75] The reproducibility of the image analysis showed no statistically significant bias suggesting that the determination of the immune cell density does not vary considerably between graders.[74,75] There was also no significant difference between eyes.[75] This inter-grader consistency is supported by the ICCs for the epithelial density and for the stromal density,[74] and concordance correlation coefficient (Table 4).[75]

Clinical Validation—The EIC density has been reported to be increased in MGD, with a cut-off of 195.8 cells/mm^2 which shows 94% sensitivity and 92% specificity suggest that EIC density could be used as a diagnostic biomarker to differentiate MGD from normal patients (Table 4).[75] In treatment studies there was a significant reduction in inflammatory cell density within the eyelid margin in groups treated with anti-inflammatory therapy compared to those without this treatment.[72,169]

In summary, EIC density and SIC density detected by IVCM exhibit excellent intra/interobserver agreement with a high sensitivity and specificity, which makes it a good candidate as a diagnostic biomarker. Decreases in the inflammatory cell density by treatment suggest that they can be useful as a pharmacodynamics biomarker.

Assessment of Corneal Nerve Alterations by IVCM

The cornea is the most densely innervated tissue in the human body, and this high density of nerves is crucial for the protection of the eye through reflex blinking, maintenance of corneal epithelial integrity and regulation of wound healing.[179,180] Over the last years, IVCM has shown the capability of assessing the corneal subbasal nerve plexus (Fig. 6a) [179,181] and the following total, trunk and branch nerve density and length (Fig. 6 b,c), tortuosity (Fig. 6d), beading (Fig. 6e), nerve reflectivity and thickness (Fig. 6f), and microneuromas (Fig. 6f) have been used to evaluate corneal nerve alterations.[182-185]

Analytical Validation

Total, trunk and branch nerve density and length—The normal range for nerve fiber length has been reported between 17.1-31.7 mm/mm^2 and 28.8-38.3 numbers/mm^2 for nerve density (Table 4).[143,162,179,182,183,185-189] The range of nerve branching density was reported between 37.2-120.0 numbers/mm^2 in healthy individuals.[182,189] Nerve fiber length has been most extensively reported in the literature with moderate to excellent intra- and inter-grader ICCs (Table 4).[182,183,189-191] In diabetes mellitus, the intra-grader repeatability was good for nerve density and excellent for nerve fiber length.[189] Also, they have shown no significant bias or trends with adequate CoV (<20%).[182,183] Software with automated image analysis for nerve fiber length is currently being used and shows a good inter-grader reproducibility (ICC = 0.870-0.890), however performed consistently lower measurements (−6.7mm/mm^2) when compared to manual assessment.[182,183] However, it was reported that automated analysis might exclude nerve segments from slightly oblique images, images with mild pressure artifacts and short nerves with reduced contrast and might include some DCs as nerves,[192] but still should provide compatible results with manual tracing.[192] While data on nerve density are promising, additional validation for nerve density and branching are required.[182,183,185,192] For instance, some research groups quantify nerve branches by the branching points, while other groups quantify according to the branch length.[185]

Tortuosity—Nerve tortuosity is a morphological parameter of the corneal subbasal nerves that have been assessed by IVCM (Fig. 6d,e). The average normal value for tortuosity is reported as 1.1 grade (grade range 0-4) and tortuosity coefficient, a unitless measure that reflects the degree of curvature of nerve fibres, was reported as 20.0-38.2 in healthy individuals.[179,193,194] The intra-grader and inter-grader ICC values for tortuosity showed a wide difference between studies (Table 4).[182,190,194]

Beading—Subbasal nerve beading frequency varied from 90-198 beads/mm in healthy individuals.[187,195,196] For beading (Fig. 6e), the intragrader ICCs were excellent- and inter-grader ICCs were good (Table 4).[182,190,194]

Nerve Reflectivity and Thickness—The thickness of the subepithelial corneal nerves ranges between 0.52 and 4.68 μm[187,196,197] and reflectivity grade was 1.1-2.6 (grade range 0-4) in health.[179,195,198,199]

Microneuromas—Microneuromas are currently described as stumps of severed nerves and abrupt, hyperreflective endings of nerve fibers on IVCM and they are evaluated for their presence or absence in different diseases, especially in neuropathic corneal pain.[200-202]

Clinical Validation

The most frequent ocular conditions investigated for nerve density and length via IVCM have been DED,[64,143,147] herpes simplex keratitis (Fig. 6b),[203-205] herpes zoster ophthalmicus,[138,206] neurotrophic keratitis (Fig. 6c)[207] neuropathic corneal pain and post-refractive surgery;[184,200,201] however, other anterior segment diseases, such as keratoconus,[208] corneal dystrophies,[139] and vernal[209] and atopic keratoconjunctivitis[210] and limbal stem cell deficiency[211,212] have also been studied. Furthermore, systemic diseases including endocrine disorders, such as diabetes[213,214] and thyroid diseases,[215] multiple sclerosis,[160,216,217] Parkinson disease,[216,218] small fiber neuropathy[219] graft versus host disease[171] and mucous membrane pemphigoid[157] have also been investigated.

Total, trunk and branch nerve density and length—Most of the previous studies reported decreased corneal nerve density and length per frame in most ocular and systemic conditions.[185] The cut off values of nerve density and nerve length to differentiate normal controls from DED were determined as 36.5 nerves/mm^2 with 80.2% sensitivity and 85.0% specificity and 12.5 mm/mm^2 with 81.9% sensitivity and 85.0% specificity, respectively.[220] In DED, nerve density and corneal sensation showed conflicting results where some reported negative and others positive correlations.[147,221,222] However, nerve density was negatively correlated with symptom severity[143,223] and fluorescein corneal staining and positively correlated with corneal sensation in DED.[221,224] Furthermore, DED patients with high nerve density responded to treatment better than the patients with low nerve density suggesting it can be used as a predictive biomarker for treatment stratification and likelihood of treatment response.[162] Moreover, increased nerve density was reported as a pharmacodynamic biomarker for topical treatment in DED, such as cord blood serum and cyclosporine.[202,225,226]

Similar to DED, in herpes simplex keratitis nerve density revealed positive correlation with corneal sensitivity.[185,203,227] Furthermore, it was shown that unilateral herpes simplex and herpes zoster keratitis results in decreased nerve density compared to controls, even in the contralateral non-affected eye.[206,228] Moreover, decreased corneal nerve length has been reported in patients who developed neurotrophic keratitis after neurosurgical trigeminal damage, where IVCM assessment was proposed for all patients with trigeminal impairment.[229] The reported correlations herein support the use as a monitoring biomarker in DED, infectious keratitis and neurotrophic keratitis.

IVCM also showed nerve regeneration in DED, neuropathic corneal pain, herpes simplex keratitis, and neurotrophic keratitis with treatment, showing its potential as a pharmacodynamic biomarker.[162,202,225,230-232] In contrast, diabetes mellitus showed decreased corneal nerve density, and its negative correlation with the severity of peripheral neuropathy[233-238] and retinopathy were established.[239-242] For the diagnosis of neuropathy in diabetes the sensitivity and specificity of nerve density were 82% and 52%, respectively.

[237] In addition to correlation with diabetic peripheral complications, it was showed that reduced corneal nerve density might be present before development of those complications. [243,244] And, the negative correlation between mean nerve density and HbA1c and improvement of nerve density after good glycemic control were also reported.[236,245-247] As a result of these reports, corneal nerve density in diabetes has shown to be an important predictive and monitoring biomarker.

Tortuosity—In DED, increased tortuosity is reported consistently in numerous studies; [195,196,223] Previous studies reported increased nerve tortuosity in different subtypes of DED, which was significantly different when compared to controls.[195,196,223] Nerve tortuosity was reported positively correlated with corneal sensation and negatively correlated with fluorescein staining in dry eye.[224] Negative correlation (r= −0.179) between Schirmer's I test and nerve tortuosity is also reported. [196,198,220,248] However, some studies showed no significant correlation of nerve tortuosity with signs and symptoms.[221,223,249] Therefore, it seems that nerve tortuosity does not seem promising as a diagnostic biomarker. However, decreased nerve tortuosity with treatment was also reported in dry eye, which suggests that tortuosity may be used as a pharmacodynamic biomarker.[181,202,225,226]

In *diabetes mellitus,* increased nerve tortuosity and its correlation with the severity of peripheral neuropathy and retinopathy was established.[233-237,239,240] Different definitions of tortuosity have been used to develop some qualitative and quantitative grading scales; however, previously used grading scales still need improvement because of their subjectivity and unfeasibility for clinical use and insufficient assessment of its complex mathematical definition.[179,233] Annunziata et al developed a promising, fully automated, hybrid segmentation system to assess tortuosity objectively and definition free, which might increase our knowledge about nerve tortuosity and its correlation with clinical symptoms and signs.[250] This fully automated nerve tortuosity quantification showed a sensitivity of 51.9 - 58.8% and specificity of 81.1 - 84.7%.[250]

Beading—In DED, increased beading is reported consistently in numerous studies; [195,196,223] Number of beading were reported as 332-387/mm in Sjogren related DED and 186-323/mm and in non-Sjogren related dry eye.[195,223,224] Decreased nerve beading with topical chord serum tears and cyclosporine treatment was also reported in DED. [181,202,225,226] Thus literature about nerve beading and its change with treatment is limited. For being a biomarker it still needs to be investigated.

Reflectivity and Thickness—Nerve reflectivity and thickness did not show consistent results.[143,185] Correlation between nerve reflectivity and OSDI[143] and decrease in nerve reflectivity with topical cyclosporine treatment was also reported.[225]

Microneuromas—Microneuromas have been proposed as a tool to assist in the diagnosis of neuropathic corneal pain patients.[200,201,251,252] Microneuromas are known to be the source of ectopic spontaneous excitations in sensory fibers in patients with postsurgical pain. [253] In 2015, Aggarwal et al. first described microneuromas as stumps of severed nerves and abrupt endings of nerve fibers on IVCM and reported their presence in photoallodynia patients with, which decreased with treatment of autologous serum tears.[200] In recent study,

Aggarwal et al, showed that in neuropathic corneal pain patients with different etiologies, such as post-refractive surgery, DED, autonomic neuropathy, herpes zoster ophthalmicus and UV light exposure showed presence of neuromas in 100% of the patients and decreased to 6.25% with treatment.[201] Additionally, a more recent study showed that microneuroma presence had a 100% sensitivity and 100% specificity in differentiating DED and NCP and warrants additional validation studies in larger cohorts.[252] Due to the lack of validated biomarkers in this ill-defined disease, microneuromas detected by IVCM are currently being validated, since current studies suggest them as a diagnostic and/or monitoring biomarker in the near future.[200,201,251,254]

In summary, the nerve fiber density (total, trunk and branch) and length have been the most validated parameters to date. Other nerve parameters such as nerve tortuosity and beading require further validation and standardization of method due to their variability and subjectivity, whereas nerve reflectivity, nerve thickness require full analytical validation. In addition, the clinical value of these morphological findings is yet to be established, the exception are microneuromas that have shown to be highly prevalent and a potential biomarker in neuropathic corneal pain patients. In this context, nerve density and length are unlikely to be a diagnostic biomarker when used in isolation, but they can become a useful non-invasive biomarker to monitor the level of nerve damage and regeneration.[186] To date, clinical use of these biomarkers, most importantly in diabetic neuropathy, is focused on demonstrating severity of disease, on endpoints for treatment response, on monitoring and on predicting disease progress.

Corneal Thickness and Epithelial Thickness

Anterior segment OCT provides high-quality cross-sectional images based on the reflectivity of ocular structures through low-coherence interferometry. By performing high resolution anterior segment OCT scans on 8 meridians of the cornea, an automated software can reconstruct the cornea 3-dimensionally, generating 10-mm radius pachymetry; the latter can be further segmented to generate epithelial thickness maps by identifying the hypereflective basement membrane and surface of the epithelium (Fig. 7).[255]

Analytical Validation

The reported mean normal epithelial thickness is 50.4-53.4 μm.[256-260] When comparing ultra-high resolution ultrasound and anterior segment OCT for measuring epithelial thickness, they was close inter-grader agreement with an average measurement difference of 4 microns and 95% limits of agreement between −4.6μm and +3.2μm.[261] Epithelial thickness as measured by AS-OCT showed high repeatability for central and peripheral cornea and excellent reproducibility (Table 4).[256,259,260,262,263]

Clinical Validation

Anterior segment OCT epithelial thickness evaluation has been utilized as a diagnostic biomarker for ectasias, DED, and limbal stem cell deficiency. In cases of keratoconus, the epithelial thickness is thinner in areas overlying areas of corneal steepening[256,257] and showed a high sensitivity of 88.9% and specificity of 59.5%, with an optimal cutoff of 52

μm at the thinnest area of the cornea, in early disease (form fruste) due to the potential epithelial changes that occur prior to topographical changes.[258,264] More specifically, anterior segment OCT epithelial thickness showed high accuracy (AUC= 0.840 to 0.985) in detecting keratoconus even in form fruste cases.[256,265,266]

In keratoconus patients, the corneal epithelial thickness ranged from 40.0 μm to 51.9 μm and its parameters such as central, inferior, minimal-maximum and standard deviation showed various AUC values, however the pattern standard deviation showed 100% sensitivity and specificity in detecting keratoconus (Table 4).[256,264-266] Furthermore, the pattern standard deviation of epithelial thickness maps increased the accuracy in diagnosing subclinical keratoconus (AUC= 0.985), higher than pachymetry map-based keratoconus risk score (AUC= 0.735);[265] even in subclinical disease with normal pachymetry-based keratoconus percentage index (KISA%) values the diagnostic power was high (AUC= 0.961).

In DED[267,268] and limbal stem cell deficiency[269-271] patients have shown epithelial thickness thinning as measured by AS-OCT at the limbus and central cornea compared to controls. In limbal stem cell deficiency the corneal epithelial thickness correlated with visualization of palisades of Vogt (r= 0.82-0.89).[269,271]

The AS-OCT epithelial thickness has shown sufficient analytical validation with good repeatability and reproducibility even in diseases patients. In addition, its non-invasive and non-contact nature makes this a promising biomarker particularly for the diagnosis of keratoconus using the pattern standard deviation and should be considered for future clinical trials for early diagnosis and pre-operative screening for keratoconus. Therefore, anterior segment OCT epithelial thickness has the potential to be a good diagnostic and monitoring biomarker.

Qualitative Biomarkers

IVCM allows direct visualization of infectious pathogens and cellular changes of cornea in patients with keratitis, and provides comparable results with corneal cultures and PCR.[272] Therefore, they may be thought as diagnostic and pharmacodynamics biomarkers in demodex folliculorum blepharitis and infectious keratitis. These are different than quantitative measure described above, therefore outlined in a separate section:

Demodex Folliculorum Blepharitis

Demodex folliculorum and *D. brevis* are microscopic parasites that can infest the eyelashes and are a common cause of blepharitis. A pathognomonic finding on slit-lamp examination is collaret formation or crusts on the eyelashes, and diagnosis requires eyelash sampling with visualization of the parasites under the microscope.[273] However, performing IVCM on the eye lids/eyelash can also provide diagnosis for Demodex blepharitis since these parasites are directly seen on the eyelash and confirmed by analyzing depilated eyelashes under light microscope.[274,275] The mites are generally imaged with longitudinal section. D. brevis and D. follicularis are seen as structures with hyperreflective legs around 250 μm and 350 μm length, respectively in longitudinal sections (Fig. 8a-b).[274,275] It is possible to show these parasites inside the follicle, inside the follicle next to MG, between two eyelashes and at the

bottom of a follicle with accompanying follicle distension, epithelium hyperreflectivity, MG obstruction and reactional epithelial proliferation.[274] A prospective study has shown that sensitivity and specificity of IVCM to detect Demodex infestation based on the definition of light microscopy positive demodex were 100% and 98.8% when performed and analyzed by experienced observers.[276] Therefore, IVCM can be used in the diagnosis of ocular Demodex infestation and related structural changes. Therefore, it can be thought as a diagnostic biomarker.

Acanthamoeba Keratitis

Both cysts and trophozoites of *Acanthamoeba* can be visualized by IVCM (Fig. 8c). Cysts are seen highly reflective double-walled round structures in 10-25 μm diameter. Trophozoites appear as hyperreflective ovoid or irregular structures with pseudopods measuring 25-40 μm.[272,277,278] The accuracy to detect on IVCM with experienced observers on culture positive or light microscopy positive ulcers was 94.8%.[279] The sensitivity and specificity of IVCM to diagnose *Acanthamoeba* are reported 69.7-100% and 84.0-100%, respectively.[278,280] Thus, IVCM can provide fast and definite diagnosis for *Acanthomoeba* keratitis and may serve as a diagnostic biomarker for this disease.

Fungal Keratitis

Aspergillus sp and Fusarium sp are the most common pathogens of fungal keratitis. Aspergillus spp was described as 200-400 μm hyperreflective structures with 5-10 μm septate hyphae with 45° dichotomous branches (Fig. 8d); conversely, Fusarium spp was described with branching at 90° in most of the IVCM studies on infectious keratitis.[281,282] However, in a recent study, the mean branching angle was measured as 59.7° and 63.3° for Fusarium spp and Aspergillus spp, respectively and the same study reported that dichotomous branching can be rarely seen with IVCM.[283] Moreover, previous studies reported that IVCM is not only a diagnostic tool for infectious keratitis (accuracy of 94.8%) but also useful and valuable to follow treatment response and early detection of relapse in severe cases.[279,284,285] The reported sensitivity and specificity of IVCM for fungus filaments detection were 71.4-94% and 78-81.4%, respectively.[278,279,281,282]

In summary, IVCM can serve as a diagnostic biomarker for fungal keratitis. Moreover, when it is applied to assess treatment response, it may be helpful as a monitoring biomarker.

Summary

This review assessed the current state of NITBUT, TMH, TMA, MG dropout, ocular redness grading scores, inflammatory cell density, DC density, nerve density, and epithelial thickness to as potential optical biomarkers in the scope of analytical and clinical validation. To date, none of the parameters can be described as a certain biomarker based on biomarker development processes shown in Table 1 and 2. However, NITBUT, TMH and TMA may become diagnostic biomarkers for DED once analytical and clinical validation are completed. Furthermore, DC density and palpebral immune cell density reflect the state of ocular surface inflammation with a good sensitivity and specificity. Although they cannot differentiate a specific disease, ocular inflammation can be diagnosed by these parameters

and treatment response to anti-inflammatory theraies can be evaluated, highlighting their potential to additionally become monitoring and pharmacodynamics biomarkers. Like inflammatory cell density, nerve density may not address a specific disease but can be a promising candidate for being a monitoring or pharmacodynamic biomarker in ocular (DED, neurotrophic keratitis, neuropathic corneal pain etc.) and systemic conditions, such as in diabetes. Lastly, epithelial thickness measured by AS-OCT has a high potential to be a diagnostic and monitoring biomarker for keratoconus patients.

Future Directions

The imaging parameters discussed herein have been summarized in Table 3 and are new or emerging tools that may provide potential biomarkers for ocular surface diseases. There is a strong need for analytical or further clinical validation to provide the necessary evidence (or fit of purpose) to qualify these imaging parameters for clinical use. The NIBUT has had extensive analytical validation supported by many groups. This has provided clinicians with an understanding of its limitations, which are lack of reproducibility across devices and larger variation at higher values. In addition, NIBUT has shown diagnostic potential via clinical validation. More extensive clinical validation is necessary if NIBUT is to be used as any other biomarker type. These additional clinical validations are likely to be pursued if NIBUT is used more widely within the clinic. To date, most studies appear to favor the traditional fluorescein TBUT.

The ocular redness grading scales have been extensively validated and implemented in clinical practice. However, most of the recent, automated, more reliable and continuous grading methods presented herein have not reached the same level of evidence for clinical trials as previous illustrative scales; in part due to the high costs of these high-resolution/ specialized devices or computer software development.[108] New methods to quantify ocular redness or the use of automated analysis, such as ORI, are warranted with the latter showing promising results that require further clinical validation. Future clinical studies to address this issue ideally should present a practical approach with an objective continuous scale, low cost, high repeatability and reliability, high sensitivity to detect small incremental changes and should be comparable to previous studies.

Moreover, IVCM has emerged as an important non-invasive tool for ocular surface diseases. More specifically, the microscopic visualization of DCs and subbasal nerve plexus of the cornea has provided a novel approach to detect inflammation and nerve abnormalities of the ocular surface that could be secondary to systemic diseases such as in diabetes mellitus. Therefore, as highlighted in this review, the biomarkers with the highest level of evidence to date are DC density to diagnose and monitor inflammation of the ocular surface, particularly in DED, and total nerve density to monitor severity or progression for diabetes and neurotrophic keratitis

The use of artificial intelligence in ophthalmology is rapidly growing and might greatly impact imaging analysis in the near future.[286] Most recently, its use on IVCM image analysis has been shown to be capable of detecting DCs and micro-neuromas in a fast and automated process with high sensitivity (66.0% and 91.3%, respectively) and specificity (99.0% and 90.0%, respectively), further facilitating its implementation as a complimentary

tool for ophthalmologists in research and clinical settings.[141,287] There is growing evidence of the neuro-immune crosstalk that occurs in the cornea, highlighting the importance of these non-invasive biomarkers for monitoring in ocular surface disease.[140137]

Overall, the epithelial thickness maps as measured by anterior segment OCT is a novel reliable parameter to differentiate diseased corneas from healthy corneas.[263] Since many ocular surface diseases affect the corneal epithelium, either directly or indirectly, assessing changes to this layer can be a promising monitoring or predictive biomarker for conditions such as keratoconus. Nevertheless, studies confirming how the degree of inflammation interferes with the epithelial thickness are warranted, as the former can be a confounding factor when establishing diagnostic thickness cut-off values. Furthermore, advances in OCT technology with novel applications for anterior segment are emerging. In particular, *en face* anterior segment OCT and anterior segment OCT angiography have been explored in ocular surface diseases and are capable of imaging corneal neovascularization and conjunctival-limbal vessels.[5,288,289] For example, in limbal stem cell deficiency anterior segment OCT angiography has shown an increase in corneal vessel extension and depth in disease correlating to disease severity.[290] In conjunctival tumors, the anterior segment OCT lesion features as well as its vascularization on anterior segment OCT angiography were used to differentiate benign from malignant tumors.[291] The advantage of non-invasively providing quantitative parameters of the ocular surface blood flow makes anterior segment OCT angiography a promising tool for diagnosis and monitoring.

Supplementary Material

Refer to Web version on PubMed Central for supplementary material.

Acknowledgements

The authors would like to thank Mr. Nicholas Pondelis for his assistance in the IVCM figures.

Funding: Tufts Medical Center Institutional Support, Heidelberg Imaging Fellowship, NIH-R01-EY029602.

REFERENCES

1. BEST (Biomarkers, EndpointS, and other Tools) Resource. Silver Spring (MD)2016.
2. Busanello A, Santucci D, Bonini S, Micera A. Review: Environmental impact on ocular surface disorders: Possible epigenetic mechanism modulation and potential biomarkers. Ocul Surf. 2017;15(4):680–687. [PubMed: 28572031]
3. Rassi DM, De Paiva CS, Dias LC, et al. Review: MicroRNAS in ocular surface and dry eye diseases. Ocul Surf. 2017;15(4):660–669. [PubMed: 28483646]
4. Hagan S Biomarkers of ocular surface disease using impression cytology. Biomark Med. 2017;11(12):1135–1147. [PubMed: 29182030]
5. Kessler LG, Barnhart HX, Buckler AJ, et al. The emerging science of quantitative imaging biomarkers terminology and definitions for scientific studies and regulatory submissions. Stat Methods Med Res. 2015;24(1):9–26. [PubMed: 24919826]
6. Abramson RG, Burton KR, Yu JP, et al. Methods and challenges in quantitative imaging biomarker development. Acad Radiol. 2015;22(1):25–32. [PubMed: 25481515]
7. Kallarackal GU, Ansari EA, Amos N, Martin JC, Lane C, Camilleri JP. A comparative study to assess the clinical use of Fluorescein Meniscus Time (FMT) with Tear Break up Time (TBUT) and

Schirmer's tests (ST) in the diagnosis of dry eyes. Eye (Lond). 2002;16(5):594–600. [PubMed: 12194075]

8. Begley CG, Chalmers RL, Abetz L, et al. The relationship between habitual patient-reported symptoms and clinical signs among patients with dry eye of varying severity. Invest Ophthalmol Vis Sci. 2003;44(11):4753–4761. [PubMed: 14578396]
9. Craig JP, Nichols KK, Akpek EK, et al. TFOS DEWS II Definition and Classification Report. Ocul Surf. 2017;15(3):276–283. [PubMed: 28736335]
10. King-Smith PE, Begley CG, Braun RJ. Mechanisms, imaging and structure of tear film breakup. Ocul Surf. 2018;16(1):4–30. [PubMed: 28935579]
11. Lemp MA. Breakup of the tear film. Int Ophthalmol Clin. 1973;13(1):97–102. [PubMed: 4724266]
12. Marquardt RS, R.; Christ T Modification of Tear Film Break-up Time Test for Increased Reliability The Preocular Tear Film in Health, Disease and Contact Lens Wear. Lubbock, TX1986:57–63.
13. Cho P, Brown B, Chan I, Conway R, Yap M. Reliability of the tear break-up time technique of assessing tear stability and the locations of the tear break-up in Hong Kong Chinese. Optom Vis Sci. 1992;69(11):879–885. [PubMed: 1454305]
14. Korb DR, Greiner JV, Herman J. Comparison of fluorescein break-up time measurement reproducibility using standard fluorescein strips versus the Dry Eye Test (DET) method. Cornea. 2001;20(8):811–815. [PubMed: 11685057]
15. Nichols KK, Mitchell GL, Zadnik K. The repeatability of clinical measurements of dry eye. Cornea. 2004;23(3):272–285. [PubMed: 15084861]
16. Mooi JK, Wang MTM, Lim J, Muller A, Craig JP. Minimising instilled volume reduces the impact of fluorescein on clinical measurements of tear film stability. Cont Lens Anterior Eye. 2017;40(3):170–174. [PubMed: 28173986]
17. Best N, Drury L, Wolffsohn JS. Clinical evaluation of the Oculus Keratograph. Cont Lens Anterior Eye. 2012;35(4):171–174. [PubMed: 22542606]
18. Hong J, Sun X, Wei A, et al. Assessment of tear film stability in dry eye with a newly developed keratograph. Cornea. 2013;32(5):716–721. [PubMed: 23132457]
19. Gumus K, Crockett CH, Rao K, et al. Noninvasive assessment of tear stability with the tear stability analysis system in tear dysfunction patients. Invest Ophthalmol Vis Sci. 2011;52(1):456–461. [PubMed: 20631241]
20. Abdelfattah NS, Dastiridou A, Sadda SR, Lee OL. Noninvasive Imaging of Tear Film Dynamics in Eyes With Ocular Surface Disease. Cornea. 2015;34 Suppl 10:S48–52. [PubMed: 26226477]
21. Wolffsohn JS, Arita R, Chalmers R, et al. TFOS DEWS II Diagnostic Methodology report. Ocul Surf. 2017;15(3):539–574. [PubMed: 28736342]
22. Jiang Y, Ye H, Xu J, Lu Y. Noninvasive Keratograph assessment of tear film break-up time and location in patients with age-related cataracts and dry eye syndrome. J Int Med Res. 2014;42(2):494–502. [PubMed: 24445695]
23. Downie LE. Automated Tear Film Surface Quality Breakup Time as a Novel Clinical Marker for Tear Hyperosmolarity in Dry Eye Disease. Invest Ophthalmol Vis Sci. 2015;56(12):7260–7268. [PubMed: 26544794]
24. Lan W, Lin L, Yang X, Yu M. Automatic noninvasive tear breakup time (TBUT) and conventional fluorescent TBUT. Optom Vis Sci. 2014;91(12):1412–1418. [PubMed: 25343685]
25. Markoulli M, Duong TB, Lin M, Papas E. Imaging the Tear Film: A Comparison Between the Subjective Keeler Tearscope-Plus and the Objective Oculus(R) Keratograph 5M and LipiView(R) Interferometer. Curr Eye Res. 2018;43(2):155–162. [PubMed: 29135324]
26. Tian L, Qu JH, Zhang XY, Sun XG. Repeatability and Reproducibility of Noninvasive Keratograph 5M Measurements in Patients with Dry Eye Disease. J Ophthalmol. 2016;2016:8013621. [PubMed: 27190639]
27. Cox SM, Nichols KK, Nichols JJ. Agreement between Automated and Traditional Measures of Tear Film Breakup. Optom Vis Sci. 2015;92(9):e257–263. [PubMed: 26154689]
28. Lee R, Yeo S, Aung HT, Tong L. Agreement of noninvasive tear break-up time measurement between Tomey RT-7000 Auto Refractor-Keratometer and Oculus Keratograph 5M. Clin Ophthalmol. 2016;10:1785–1790. [PubMed: 27695283]

29. Mengher LS, Pandher KS, Bron AJ. Non-invasive tear film break-up time: sensitivity and specificity. Acta Ophthalmol (Copenh). 1986;64(4):441–444. [PubMed: 3776509]
30. Pult H, Purslow C, Murphy PJ. The relationship between clinical signs and dry eye symptoms. Eye (Lond). 2011;25(4):502–510. [PubMed: 21252949]
31. Wang MTM, Xue AL, Craig JP. Screening utility of a rapid non-invasive dry eye assessment algorithm. Cont Lens Anterior Eye. 2018.
32. Yamaguchi M, Sakane Y, Kamao T, et al. Noninvasive Dry Eye Assessment Using High-Technology Ophthalmic Examination Devices. Cornea. 2016;35 Suppl 1:S38–S48. [PubMed: 27661073]
33. Bilkhu PS, Naroo SA, Wolffsohn JS. Randomised masked clinical trial of the MGDRx EyeBag for the treatment of meibomian gland dysfunction-related evaporative dry eye. Br J Ophthalmol. 2014;98(12):1707–1711. [PubMed: 24997178]
34. Prabhasawat P, Tesavibul N, Mahawong W. A randomized double-masked study of 0.05% cyclosporine ophthalmic emulsion in the treatment of meibomian gland dysfunction. Cornea. 2012;31(12):1386–1393. [PubMed: 23135530]
35. Ngo W, Srinivasan S, Jones L. An Eyelid Warming Device for the Management of Meibomian Gland Dysfunction. J Optom. 2019;12(2):120–130. [PubMed: 30341026]
36. Johnson ME, Murphy PJ. The agreement and repeatability of tear meniscus height measurement methods. Optom Vis Sci. 2005;82(12):1030–1037. [PubMed: 16357644]
37. Shen M, Li J, Wang J, et al. Upper and lower tear menisci in the diagnosis of dry eye. Invest Ophthalmol Vis Sci. 2009;50(6):2722–2726. [PubMed: 19218609]
38. Wei A, Le Q, Hong J, Wang W, Wang F, Xu J. Assessment of Lower Tear Meniscus. Optom Vis Sci. 2016;93(11):1420–1425. [PubMed: 27668635]
39. Arriola-Villalobos P, Fernandez-Vigo JI, Diaz-Valle D, Peraza-Nieves JE, Fernandez-Perez C, Benitez-Del-Castillo JM. Assessment of lower tear meniscus measurements obtained with Keratograph and agreement with Fourier-domain optical-coherence tomography. Br J Ophthalmol. 2015;99(8):1120–1125. [PubMed: 25677670]
40. Canan H, Altan-Yaycioglu R, Ulas B, Sizmaz S, Coban-Karatas M. Interexaminer reproducibility of optical coherence tomography for measuring the tear film meniscus. Curr Eye Res. 2014;39(12):1145–1150. [PubMed: 24749829]
41. Chen Q, Wang J, Shen M, et al. Lower volumes of tear menisci in contact lens wearers with dry eye symptoms. Invest Ophthalmol Vis Sci. 2009;50(7):3159–3163. [PubMed: 19279314]
42. Ibrahim OM, Dogru M, Takano Y, et al. Application of visante optical coherence tomography tear meniscus height measurement in the diagnosis of dry eye disease. Ophthalmology. 2010;117(10):1923–1929. [PubMed: 20605216]
43. Fukuda R, Usui T, Miyai T, Yamagami S, Amano S. Tear meniscus evaluation by anterior segment swept-source optical coherence tomography. Am J Ophthalmol. 2013;155(4):620–624, 624 e621-622. [PubMed: 23317654]
44. Altan-Yaycioglu R, Sizmaz S, Canan H, Coban-Karatas M. Optical coherence tomography for measuring the tear film meniscus: correlation with schirmer test and tear-film breakup time. Curr Eye Res. 2013;38(7):736–742. [PubMed: 23489244]
45. Podoleanu A Principles of En Face Optical Coherence Tomography: Real Time and Post-processing En Face Imaging in Ophthalmology Clinical En Face OCT Atlas. New Delhi, India: Jaypee Brothers Medical Publishers Ltd; 2013:5–14.
46. Lange AP, Sadjadi R, Saeedi J, Lindley J, Costello F, Traboulsee AL. Time-Domain and Spectral-Domain Optical Coherence Tomography of Retinal Nerve Fiber Layer in MS Patients and Healthy Controls. J Ophthalmol. 2012;2012:564627. [PubMed: 22685631]
47. Miller AR, Roisman L, Zhang Q, et al. Comparison Between Spectral-Domain and Swept-Source Optical Coherence Tomography Angiographic Imaging of Choroidal Neovascularization. Invest Ophthalmol Vis Sci. 2017;58(3):1499–1505. [PubMed: 28273316]
48. Imamura H, Tabuchi H, Nakakura S, Nagasato D, Baba H, Kiuchi Y. Usability and reproducibility of tear meniscus values generated via swept-source optical coherence tomography and the slit lamp with a graticule method. Int Ophthalmol. 2018;38(2):679–686. [PubMed: 28393321]

49. Smith J, Nichols KK, Baldwin EK. Current patterns in the use of diagnostic tests in dry eye evaluation. Cornea. 2008;27(6):656–662. [PubMed: 18580256]
50. Golding TR, Bruce AS, Mainstone JC. Relationship between tear-meniscus parameters and tear-film breakup. Cornea. 1997;16(6):649–661. [PubMed: 9395875]
51. Chan HH, Zhao Y, Tun TA, Tong L. Repeatability of tear meniscus evaluation using spectral-domain Cirrus(R) HD-OCT and time-domain Visante(R) OCT. Cont Lens Anterior Eye. 2015;38(5):368–372. [PubMed: 25956571]
52. Tung CI, Perin AF, Gumus K, Pflugfelder SC. Tear meniscus dimensions in tear dysfunction and their correlation with clinical parameters. Am J Ophthalmol. 2014;157(2):301–310 e301. [PubMed: 24315297]
53. Tittler EH, Bujak MC, Nguyen P, et al. Between-grader repeatability of tear meniscus measurements using Fourier-domain OCT in patients with dry eye. Ophthalmic Surg Lasers Imaging. 2011;42(5):423–427. [PubMed: 21899246]
54. Qiu X, Gong L, Lu Y, Jin H, Robitaille M. The diagnostic significance of Fourier-domain optical coherence tomography in Sjogren syndrome, aqueous tear deficiency and lipid tear deficiency patients. Acta Ophthalmol. 2012;90(5):e359–366. [PubMed: 22568661]
55. El-Fayoumi D, Youssef MM, Khafagy MM, Badr El Dine N, Gaber W. Assessment of Corneal and Tear Film Parameters in Rheumatoid Arthritis Patients Using Anterior Segment Spectral Domain Optical Coherence Tomography. Ocul Immunol Inflamm. 2018;26(4):632–638. [PubMed: 28026971]
56. Akiyama-Fukuda R, Usui T, Yoshida T, Yamagami S. Evaluation of Tear Meniscus Dynamics Using Anterior Segment Swept-Source Optical Coherence Tomography After Topical Solution Instillation for Dry Eye. Cornea. 2016;35(5):654–658. [PubMed: 26989953]
57. Carracedo G, Pastrana C, Serramito M, Rodriguez-Pomar C. Evaluation of tear meniscus by optical coherence tomography after different sodium hyaluronate eyedrops instillation. Acta Ophthalmol. 2019;97(2):e162–e169. [PubMed: 30280515]
58. Ibrahim OM, Dogru M, Kojima T, et al. OCT assessment of tear meniscus after punctal occlusion in dry eye disease. Optom Vis Sci. 2012;89(5):E770–776. [PubMed: 22466101]
59. Nagahara Y, Koh S, Maeda N, Nishida K, Watanabe H. Prominent Decrease of Tear Meniscus Height With Contact Lens Wear and Efficacy of Eye Drop Instillation. Eye Contact Lens. 2015;41(5):318–322. [PubMed: 25839348]
60. Nagahara Y, Koh S, Nishida K, Watanabe H. Prolonged increase in tear meniscus height by 3% diquafosol ophthalmic solution in eyes with contact lenses. Clin Ophthalmol. 2015;9:1029–1031. [PubMed: 26089634]
61. Geerling G, Tauber J, Baudouin C, et al. The international workshop on meibomian gland dysfunction: report of the subcommittee on management and treatment of meibomian gland dysfunction. Invest Ophthalmol Vis Sci. 2011;52(4):2050–2064. [PubMed: 21450919]
62. Villani E, Magnani F, Viola F, et al. In vivo confocal evaluation of the ocular surface morpho-functional unit in dry eye. Optom Vis Sci. 2013;90(6):576–586. [PubMed: 23670123]
63. Efron N, Al-Dossari M, Pritchard N. In vivo confocal microscopy of the bulbar conjunctiva. Clin Exp Ophthalmol. 2009;37(4):335–344. [PubMed: 19594558]
64. Alhatem A, Cavalcanti B, Hamrah P. In vivo confocal microscopy in dry eye disease and related conditions. Semin Ophthalmol. 2012;27(5-6):138–148. [PubMed: 23163268]
65. Agnifili L, Fasanella V, Costagliola C, et al. In vivo confocal microscopy of meibomian glands in glaucoma. Br J Ophthalmol. 2013;97(3):343–349. [PubMed: 23269683]
66. Wei Q, Le Q, Hong J, Xiang J, Wei A, Xu J. In vivo confocal microscopy of meibomian glands and palpebral conjunctiva in vernal keratoconjunctivitis. Indian J Ophthalmol. 2015;63(4):327–330. [PubMed: 26044472]
67. Zhao H, Chen JY, Wang YQ, Lin ZR, Wang S. In vivo Confocal Microscopy Evaluation of Meibomian Gland Dysfunction in Dry Eye Patients with Different Symptoms. Chin Med J (Engl). 2016;129(21):2617–2622. [PubMed: 27779170]
68. Fasanella V, Agnifili L, Mastropasqua R, et al. In Vivo Laser Scanning Confocal Microscopy of Human Meibomian Glands in Aging and Ocular Surface Diseases. Biomed Res Int. 2016;2016:7432131. [PubMed: 27047965]

69. Villani E, Beretta S, De Capitani M, Galimberti D, Viola F, Ratiglia R. In vivo confocal microscopy of meibomian glands in Sjogren's syndrome. Invest Ophthalmol Vis Sci. 2011;52(2):933–939. [PubMed: 21169534]
70. Villani E, Ceresara G, Beretta S, Magnani F, Viola F, Ratiglia R. In vivo confocal microscopy of meibomian glands in contact lens wearers. Invest Ophthalmol Vis Sci. 2011;52(8):5215–5219. [PubMed: 21571676]
71. Matsumoto Y, Sato EA, Ibrahim OM, Dogru M, Tsubota K. The application of in vivo laser confocal microscopy to the diagnosis and evaluation of meibomian gland dysfunction. Mol Vis. 2008;14:1263–1271. [PubMed: 18618006]
72. Matsumoto Y, Shigeno Y, Sato EA, et al. The evaluation of the treatment response in obstructive meibomian gland disease by in vivo laser confocal microscopy. Graefes Arch Clin Exp Ophthalmol. 2009;247(6):821–829. [PubMed: 19101718]
73. Villani E, Garoli E, Canton V, Pichi F, Nucci P, Ratiglia R. Evaluation of a novel eyelid-warming device in meibomian gland dysfunction unresponsive to traditional warm compress treatment: an in vivo confocal study. Int Ophthalmol. 2015;35(3):319–323. [PubMed: 24752646]
74. Qazi Y, Kheirkhah A, Blackie C, et al. In vivo detection of clinically non-apparent ocular surface inflammation in patients with meibomian gland dysfunction-associated refractory dry eye symptoms: a pilot study. Eye (Lond). 2015;29(8):1099–1110. [PubMed: 26088680]
75. Qazi Y, Kheirkhah A, Blackie C, et al. Clinically Relevant Immune-Cellular Metrics of Inflammation in Meibomian Gland Dysfunction. Invest Ophthalmol Vis Sci. 2018;59(15):6111–6123. [PubMed: 30592499]
76. Ibrahim OM, Matsumoto Y, Dogru M, et al. In vivo confocal microscopy evaluation of meibomian gland dysfunction in atopic-keratoconjunctivitis patients. Ophthalmology. 2012;119(10):1961–1968. [PubMed: 22717457]
77. Ibrahim OM, Matsumoto Y, Dogru M, et al. The efficacy, sensitivity, and specificity of in vivo laser confocal microscopy in the diagnosis of meibomian gland dysfunction. Ophthalmology. 2010;117(4):665–672. [PubMed: 20189653]
78. Wei A, Hong J, Sun X, Xu J. Evaluation of age-related changes in human palpebral conjunctiva and meibomian glands by in vivo confocal microscopy. Cornea. 2011;30(9):1007–1012. [PubMed: 21436687]
79. Zhou S, Robertson DM. Wide-Field In Vivo Confocal Microscopy of Meibomian Gland Acini and Rete Ridges in the Eyelid Margin. Invest Ophthalmol Vis Sci. 2018;59(10):4249–4257. [PubMed: 30128496]
80. Arita R, Itoh K, Inoue K, Amano S. Noncontact infrared meibography to document age-related changes of the meibomian glands in a normal population. Ophthalmology. 2008;115(5):911–915. [PubMed: 18452765]
81. Nichols JJ, Berntsen DA, Mitchell GL, Nichols KK. An assessment of grading scales for meibography images. Cornea. 2005;24(4):382–388. [PubMed: 15829792]
82. Pult H, Riede-Pult B. Comparison of subjective grading and objective assessment in meibography. Cont Lens Anterior Eye. 2013;36(1):22–27. [PubMed: 23108007]
83. Tomlinson A, Bron AJ, Korb DR, et al. The international workshop on meibomian gland dysfunction: report of the diagnosis subcommittee. Invest Ophthalmol Vis Sci. 2011;52(4):2006–2049. [PubMed: 21450918]
84. Pult H, Riede-Pult BH, Nichols JJ. Relation between upper and lower lids' meibomian gland morphology, tear film, and dry eye. Optom Vis Sci. 2012;89(3):E310–315. [PubMed: 22246333]
85. Daniel E, Maguire MG, Pistilli M, et al. Grading and baseline characteristics of meibomian glands in meibography images and their clinical associations in the Dry Eye Assessment and Management (DREAM) study. Ocul Surf. 2019.
86. Hwang HS, Xie Y, Koudouna E, et al. Light transmission/absorption characteristics of the meibomian gland. Ocul Surf. 2018;16(4):448–453. [PubMed: 30297027]
87. Kim HM, Eom Y, Song JS. The Relationship Between Morphology and Function of the Meibomian Glands. Eye Contact Lens. 2018;44(1):1–5. [PubMed: 27755288]
88. Ban Y, Shimazaki-Den S, Tsubota K, Shimazaki J. Morphological evaluation of meibomian glands using noncontact infrared meibography. Ocul Surf. 2013;11(1):47–53. [PubMed: 23321359]

89. Maskin SL, Testa WR. Infrared Video Meibography of Lower Lid Meibomian Glands Shows Easily Distorted Glands: Implications for Longitudinal Assessment of Atrophy or Growth Using Lower Lid Meibography. Cornea. 2018;37(10):1279–1286. [PubMed: 30067535]

90. Wong S, Srinivasan S, Murphy PJ, Jones L. Comparison of meibomian gland dropout using two infrared imaging devices. Cont Lens Anterior Eye. 2018.

91. Ngo W, Srinivasan S, Schulze M, Jones L. Repeatability of grading meibomian gland dropout using two infrared systems. Optom Vis Sci. 2014;91(6):658–667. [PubMed: 24830370]

92. Arita R, Suehiro J, Haraguchi T, Shirakawa R, Tokoro H, Amano S. Objective image analysis of the meibomian gland area. Br J Ophthalmol. 2014;98(6):746–755. [PubMed: 23813417]

93. Dogan AS, Kosker M, Arslan N, Gurdal C. Interexaminer Reliability of Meibography: Upper or Lower Eyelid? Eye Contact Lens. 2018;44(2):113–117. [PubMed: 27466721]

94. Arita R, Itoh K, Maeda S, Maeda K, Tomidokoro A, Amano S. Efficacy of diagnostic criteria for the differential diagnosis between obstructive meibomian gland dysfunction and aqueous deficiency dry eye. Jpn J Ophthalmol. 2010;54(5):387–391. [PubMed: 21052898]

95. Arita R, Itoh K, Maeda S, et al. Proposed diagnostic criteria for obstructive meibomian gland dysfunction. Ophthalmology. 2009;116(11):2058–2063 e2051. [PubMed: 19744718]

96. Turnbull PRK, Misra SL, Craig JP. Comparison of treatment effect across varying severities of meibomian gland dropout. Cont Lens Anterior Eye. 2018;41(1):88–92. [PubMed: 28974425]

97. Leibowitz HM. The red eye. N Engl J Med. 2000;343(5):345–351. [PubMed: 10922425]

98. Sethuraman U, Kamat D. The red eye: evaluation and management. Clin Pediatr (Phila). 2009;48(6):588–600. [PubMed: 19357422]

99. Cronau H, Kankanala RR, Mauger T. Diagnosis and management of red eye in primary care. Am Fam Physician. 2010;81(2):137–144. [PubMed: 20082509]

100. Efron N Grading scales for contact lens complications. Ophthalmic Physiol Opt. 1998;18(2):182–186. [PubMed: 9692040]

101. Terry RL, Schnider CM, Holden BA, et al. CCLRU standards for success of daily and extended wear contact lenses. Optom Vis Sci. 1993;70(3):234–243. [PubMed: 8483586]

102. Efron N, Morgan PB, Katsara SS. Validation of grading scales for contact lens complications. Ophthalmic Physiol Opt. 2001;21(1):17–29. [PubMed: 11220037]

103. Amparo F, Yin J, Di Zazzo A, et al. Evaluating Changes in Ocular Redness Using a Novel Automated Method. Transl Vis Sci Technol. 2017;6(4):13.

104. Chong E, Simpson T, Fonn D. The repeatability of discrete and continuous anterior segment grading scales. Optom Vis Sci. 2000;77(5):244–251. [PubMed: 10831214]

105. Papas EB. Key factors in the subjective and objective assessment of conjunctival erythema. Invest Ophthalmol Vis Sci. 2000;41(3):687–691. [PubMed: 10711682]

106. Peterson RC, Wolffsohn JS. Sensitivity and reliability of objective image analysis compared to subjective grading of bulbar hyperaemia. Br J Ophthalmol. 2007;91(11):1464–1466. [PubMed: 17475716]

107. Schulze MM, Jones DA, Simpson TL. The development of validated bulbar redness grading scales. Optom Vis Sci. 2007;84(10):976–983. [PubMed: 18049363]

108. Amparo F, Wang H, Emami-Naeini P, Karimian P, Dana R. The Ocular Redness Index: a novel automated method for measuring ocular injection. Invest Ophthalmol Vis Sci. 2013;54(7):4821–4826. [PubMed: 23766472]

109. Chao C, Richdale K, Jalbert I, Doung K, Gokhale M. Non-invasive objective and contemporary methods for measuring ocular surface inflammation in soft contact lens wearers - A review. Cont Lens Anterior Eye. 2017;40(5):273–282. [PubMed: 28602547]

110. Honrubia F, Garcia-Sanchez J, Polo V, de la Casa JM, Soto J. Conjunctival hyperaemia with the use of latanoprost versus other prostaglandin analogues in patients with ocular hypertension or glaucoma: a meta-analysis of randomised clinical trials. Br J Ophthalmol. 2009;93(3):316–321. [PubMed: 19019922]

111. Asbell PA, Potapova N. Effects of topical antiglaucoma medications on the ocular surface. Ocul Surf. 2005;3(1):27–40. [PubMed: 17131003]

112. Tong L, Hou AH, Wong TT. Altered expression level of inflammation-related genes and long-term changes in ocular surface after trabeculectomy, a prospective cohort study. Ocul Surf. 2018;16(4):441–447. [PubMed: 29935986]
113. McLaurin EB, Marsico NP, Ackerman SL, et al. Ocular itch relief with alcaftadine 0.25% versus olopatadine 0.2% in allergic conjunctivitis: pooled analysis of two multicenter randomized clinical trials. Adv Ther. 2014;31(10):1059–1071. [PubMed: 25260889]
114. Pucci N, Caputo R, di Grande L, et al. Tacrolimus vs. cyclosporine eyedrops in severe cyclosporine-resistant vernal keratoconjunctivitis: A randomized, comparative, double-blind, crossover study. Pediatr Allergy Immunol. 2015;26(3):256–261. [PubMed: 25712437]
115. Torkildsen G, Narvekar A, Bergmann M. Efficacy and safety of olopatadine hydrochloride 0.77% in patients with allergic conjunctivitis using a conjunctival allergen-challenge model. Clin Ophthalmol. 2015;9:1703–1713. [PubMed: 26392751]
116. Doan S, Gabison E, Chiambaretta F, Touati M, Cochereau I. Efficacy of azithromycin 1.5% eye drops in childhood ocular rosacea with phlyctenular blepharokeratoconjunctivitis. J Ophthalmic Inflamm Infect. 2013;3(1):38. [PubMed: 23514194]
117. Leonardi A, Van Setten G, Amrane M, et al. Efficacy and safety of 0.1% cyclosporine A cationic emulsion in the treatment of severe dry eye disease: a multicenter randomized trial. Eur J Ophthalmol. 2016;26(4):287–296. [PubMed: 27055414]
118. Park Y, Song JS, Choi CY, Yoon KC, Lee HK, Kim HS. A Randomized Multicenter Study Comparing 0.1%, 0.15%, and 0.3% Sodium Hyaluronate with 0.05% Cyclosporine in the Treatment of Dry Eye. J Ocul Pharmacol Ther. 2017;33(2):66–72. [PubMed: 27929721]
119. Wirta DL, Torkildsen GL, Moreira HR, et al. A Clinical Phase II Study to Assess Efficacy, Safety, and Tolerability of Waterfree Cyclosporine Formulation for Treatment of Dry Eye Disease. Ophthalmology. 2019;126(6):792–800. [PubMed: 30703441]
120. Jager MJ, Gregerson DS, Streilein JW. Regulators of immunological responses in the cornea and the anterior chamber of the eye. Eye (Lond). 1995;9 (Pt 2):241–246. [PubMed: 7556725]
121. Banchereau J, Steinman RM. Dendritic cells and the control of immunity. Nature. 1998;392(6673):245–252. [PubMed: 9521319]
122. Hamrah P, Zhang Q, Liu Y, Dana MR. Novel characterization of MHC class II-negative population of resident corneal Langerhans cell-type dendritic cells. Invest Ophthalmol Vis Sci. 2002;43(3):639–646. [PubMed: 11867578]
123. Brissette-Storkus CS, Reynolds SM, Lepisto AJ, Hendricks RL. Identification of a novel macrophage population in the normal mouse corneal stroma. Invest Ophthalmol Vis Sci. 2002;43(7):2264–2271. [PubMed: 12091426]
124. Ogawa M, Inomata T, Shiang T, Tsubota K, Murakami A. Method for selective quantification of immune and inflammatory cells in the cornea using flow cytometry. Journal of biological methods. 2018;5(4):e102. [PubMed: 31453252]
125. Knickelbein JE, Buela KA, Hendricks RL. Antigen-presenting cells are stratified within normal human corneas and are rapidly mobilized during ex vivo viral infection. Invest Ophthalmol Vis Sci. 2014;55(2):1118–1123. [PubMed: 24508792]
126. Forrester JV, Xu H, Kuffova L, Dick AD, McMenamin PG. Dendritic cell physiology and function in the eye. Immunological reviews. 2010;234(1):282–304. [PubMed: 20193026]
127. Latina M, Flotte T, Crean E, Sherwood ME, Granstein RD. Immunohistochemical staining of the human anterior segment. Evidence that resident cells play a role in immunologic responses. Arch Ophthalmol. 1988;106(1):95–99. [PubMed: 3276305]
128. Tuisku IS, Konttinen YT, Konttinen LM, Tervo TM. Alterations in corneal sensitivity and nerve morphology in patients with primary Sjogren's syndrome. Exp Eye Res. 2008;86(6):879–885. [PubMed: 18436208]
129. Mayer WJ, Mackert MJ, Kranebitter N, et al. Distribution of antigen presenting cells in the human cornea: correlation of in vivo confocal microscopy and immunohistochemistry in different pathologic entities. Curr Eye Res. 2012;37(11):1012–1018. [PubMed: 22667765]
130. Kheirkhah A, Muller R, Mikolajczak J, et al. Comparison of Standard Versus Wide-Field Composite Images of the Corneal Subbasal Layer by In Vivo Confocal Microscopy. Invest Ophthalmol Vis Sci. 2015;56(10):5801–5807. [PubMed: 26325419]

131. Zhivov A, Stave J, Vollmar B, Guthoff R. In vivo confocal microscopic evaluation of Langerhans cell density and distribution in the normal human corneal epithelium. Graefes Arch Clin Exp Ophthalmol. 2005;243(10):1056–1061. [PubMed: 15856272]

132. Mastropasqua L, Nubile M, Lanzini M, et al. Epithelial dendritic cell distribution in normal and inflamed human cornea: in vivo confocal microscopy study. Am J Ophthalmol. 2006;142(5):736–744. [PubMed: 17056357]

133. Shetty R, Sethu S, Deshmukh R, et al. Corneal Dendritic Cell Density Is Associated with Subbasal Nerve Plexus Features, Ocular Surface Disease Index, and Serum Vitamin D in Evaporative Dry Eye Disease. Biomed Res Int. 2016;2016:4369750. [PubMed: 26904676]

134. Lopez-de la Rosa A, Martin-Montanez V, Lopez-Miguel A, et al. Ocular response to environmental variations in contact lens wearers. Ophthalmic Physiol Opt. 2017;37(1):60–70. [PubMed: 28030882]

135. Nicolle P, Liang H, Reboussin E, et al. Proinflammatory Markers, Chemokines, and Enkephalin in Patients Suffering from Dry Eye Disease. Int J Mol Sci. 2018;19(4).

136. Kheirkhah A, Rahimi Darabad R, Cruzat A, et al. Corneal Epithelial Immune Dendritic Cell Alterations in Subtypes of Dry Eye Disease: A Pilot In Vivo Confocal Microscopic Study. Invest Ophthalmol Vis Sci. 2015;56(12):7179–7185. [PubMed: 26540656]

137. Yamaguchi T, Hamrah P, Shimazaki J. Bilateral Alterations in Corneal Nerves, Dendritic Cells, and Tear Cytokine Levels in Ocular Surface Disease. Cornea. 2016;35 Suppl 1:S65–S70. [PubMed: 27617877]

138. Cavalcanti BM, Cruzat A, Sahin A, Pavan-Langston D, Samayoa E, Hamrah P. In vivo confocal microscopy detects bilateral changes of corneal immune cells and nerves in unilateral herpes zoster ophthalmicus. Ocul Surf. 2018;16(1):101–111. [PubMed: 28923503]

139. Aggarwal S, Cavalcanti BM, Regali L, et al. In Vivo Confocal Microscopy Shows Alterations in Nerve Density and Dendritiform Cell Density in Fuchs' Endothelial Corneal Dystrophy. Am J Ophthalmol. 2018;196:136–144. [PubMed: 30194928]

140. Colorado LH, Markoulli M, Edwards K. The Relationship Between Corneal Dendritic Cells, Corneal Nerve Morphology and Tear Inflammatory Mediators and Neuropeptides in Healthy Individuals. Curr Eye Res. 2019:1–9.

141. Hamrah PK, N.D.; Kovler I; Cohen AB; Soferman R Deep Learning Convolutional Neural Network for the Classification and Segmentation of In Vivo Confocal Microscopy Images. ARVO Annual Meeting 2018; New Orleans, LA.

142. Hamrah P, Huq SO, Liu Y, Zhang Q, Dana MR. Corneal immunity is mediated by heterogeneous population of antigen-presenting cells. J Leukoc Biol. 2003;74(2):172–178. [PubMed: 12885933]

143. Tepelus TC, Chiu GB, Huang J, et al. Correlation between corneal innervation and inflammation evaluated with confocal microscopy and symptomatology in patients with dry eye syndromes: a preliminary study. Graefes Arch Clin Exp Ophthalmol. 2017;255(9):1771–1778. [PubMed: 28528377]

144. Villani E, Garoli E, Termine V, Pichi F, Ratiglia R, Nucci P. Corneal Confocal Microscopy in Dry Eye Treated with Corticosteroids. Optom Vis Sci. 2015;92(9):e290–295. [PubMed: 25909241]

145. Villani E, Baudouin C, Efron N, et al. In vivo confocal microscopy of the ocular surface: from bench to bedside. Curr Eye Res. 2014;39(3):213–231. [PubMed: 24215436]

146. Qazi Y, Aggarwal S, Hamrah P. Image-guided evaluation and monitoring of treatment response in patients with dry eye disease. Graefes Arch Clin Exp Ophthalmol. 2014;252(6):857–872. [PubMed: 24696045]

147. Matsumoto Y, Ibrahim OMA. Application of In Vivo Confocal Microscopy in Dry Eye Disease. Invest Ophthalmol Vis Sci. 2018;59(14):DES41–DES47. [PubMed: 30481805]

148. Liu M, Gao H, Wang T, Wang S, Li S, Shi W. An essential role for dendritic cells in vernal keratoconjunctivitis: analysis by laser scanning confocal microscopy. Clin Exp Allergy. 2014;44(3):362–370. [PubMed: 24372712]

149. Cruzat A, Schrems WA, Schrems-Hoesl LM, et al. Contralateral Clinically Unaffected Eyes of Patients With Unilateral Infectious Keratitis Demonstrate a Sympathetic Immune Response. Invest Ophthalmol Vis Sci. 2015;56(11):6612–6620. [PubMed: 26465889]

150. Yamaguchi T, Calvacanti BM, Cruzat A, et al. Correlation between human tear cytokine levels and cellular corneal changes in patients with bacterial keratitis by in vivo confocal microscopy. Invest Ophthalmol Vis Sci. 2014;55(11):7457–7466. [PubMed: 25324281]

151. Alzahrani Y, Colorado LH, Pritchard N, Efron N. Longitudinal changes in Langerhans cell density of the cornea and conjunctiva in contact lens-induced dry eye. Clin Exp Optom. 2017;100(1):33–40. [PubMed: 27353750]

152. Villani E, Sacchi M, Magnani F, et al. The Ocular Surface in Medically Controlled Glaucoma: An In Vivo Confocal Study. Invest Ophthalmol Vis Sci. 2016;57(3):1003–1010. [PubMed: 26962696]

153. Mastropasqua R, Agnifili L, Fasanella V, et al. In Vivo Distribution of Corneal Epithelial Dendritic Cells in Patients With Glaucoma. Invest Ophthalmol Vis Sci. 2016;57(14):5996–6002. [PubMed: 27820631]

154. Baghdasaryan E, Tepelus TC, Vickers LA, et al. Assessment of Corneal Changes Associated with Topical Antiglaucoma Therapy Using in vivo Confocal Microscopy. Ophthalmic Res. 2019;61(1):51–59. [PubMed: 29627838]

155. Patel DV, Zhang J, McGhee CN. In vivo confocal microscopy of the inflamed anterior segment: A review of clinical and research applications. Clin Exp Ophthalmol. 2019;47(3):334–345. [PubMed: 30953391]

156. Wu LQ, Cheng JW, Cai JP, et al. Observation of Corneal Langerhans Cells by In Vivo Confocal Microscopy in Thyroid-Associated Ophthalmopathy. Curr Eye Res. 2016;41(7):927–932. [PubMed: 26735162]

157. Tepelus TC, Huang J, Sadda SR, Lee OL. Characterization of Corneal Involvement in Eyes With Mucous Membrane Pemphigoid by In Vivo Confocal Microscopy. Cornea. 2017;36(8):933–941. [PubMed: 28399039]

158. Bitirgen G, Tinkir Kayitmazbatir E, Satirtav G, Malik RA, Ozkagnici A. In Vivo Confocal Microscopic Evaluation of Corneal Nerve Fibers and Dendritic Cells in Patients With Behcet's Disease. Front Neurol. 2018;9:204. [PubMed: 29643833]

159. Lagali NS, Badian RA, Liu X, et al. Dendritic cell maturation in the corneal epithelium with onset of type 2 diabetes is associated with tumor necrosis factor receptor superfamily member 9. Sci Rep. 2018;8(1):14248. [PubMed: 30250206]

160. Bitirgen G, Akpinar Z, Malik RA, Ozkagnici A. Use of Corneal Confocal Microscopy to Detect Corneal Nerve Loss and Increased Dendritic Cells in Patients With Multiple Sclerosis. JAMA Ophthalmol. 2017;135(7):777–782. [PubMed: 28570722]

161. Wang EF, Misra SL, Patel DV. In Vivo Confocal Microscopy of the Human Cornea in the Assessment of Peripheral Neuropathy and Systemic Diseases. Biomed Res Int. 2015;2015:951081. [PubMed: 26770980]

162. Kheirkhah A, Dohlman TH, Amparo F, et al. Effects of corneal nerve density on the response to treatment in dry eye disease. Ophthalmology. 2015;122(4):662–668. [PubMed: 25542519]

163. Akhlaq AK A; Aggarwal S; Cavalcanti B; Mueller R; Abbouda A; Salem Z; Dana R; Hamrah P Patients Enrichment for Increased Dendritiform Cells using in Vivo Confocal Microscopy Results in Improved Response to Topical Steroids in Dry Eye Disease: Results of the Therapeutic Response to Antiinflammatory agents in the Corneal Epithelium (TRACE) study ARVO Annual Meeting; 2019; Vancouver, BC.

164. Qazi YK A; Dohlman TH; Cruzat A; Cavalcanti B; Colon C; Dana R; Hamrah P Corneal Dendritic Cells as a Surrogate Biomarker of Therapeutic Efficacy in Dry Eye-Associated Corneal Inflammation. ARVO Annual Meeting Abstract; 2015; Denver, CO.

165. Cavalcanti B, Cruzat A, Q Y, et al. Contact Lens/Contact Lens solution Combinations Determine the Inflammatory Changes on the Ocular Surface: A Laser In Vivo Confocal Microscopy Study. ARVO Annual Meeting Abstract; 2012; Fort Lauderdale, FL.

166. Kataguiri PD G; Aggarwal S; Muller RT; Cavalcanti B; Qazi Y; Cruzat A; Kheirkhah A; Hamrah P Clinical Signs of Dry Eye Disease are Correlated to Peripheral Corneal Immune Cell Alterations by In Vivo Confocal Microscopy ARVO Annual Meeting 2017.

167. Dieckmann GS-R, Y.; Koseoglu ND; Jamali A; Chao C; Salem Z; Nose R; Akhlaq A; Sahin A; Cox S; Hamrah P Structural and Functional Corneal Nerve Abnormalities Indicate a

Neurosensory Origin of Contact Lens Discomfort. The Association for Research in Vision and Ophthalmology; 2019; Vancouver, BC.

168. Williams CGC, B.M.; Cruzat A; Trinidad M; Haussler-Sinangin Y; Dana R; Hamrah P In Vivo Confocal Microscopy as a Tool to Evaluate Cellular Changes in the Cornea and Conjunctiva in Ocular Allergy and Non-Allergic Ocular Inflammatory Diseases. ARVO Annual Meeting; 2012.
169. Qazi Y; Kheirkhah AD, T.H.; Amparo F; Dana R; Hamrah P Relative Efficacy of Loteprednol (Lotemax®) vs. Loteprednol-Tobramycin (Zylet®) on Corneal and Conjunctival Immune Response in Treatment of Meibomian Gland Dysfunction (MGD)-Associated Ocular Surface Inflammation: In Vivo Confocal Microscopy Results of a Phase IV Randomized Clinical Trial. ARVO Annual Meeting; 2014.
170. Kwon MS, Carnt NA, Truong NR, et al. Dendritic cells in the cornea during Herpes simplex viral infection and inflammation. Surv Ophthalmol. 2018;63(4):565–578. [PubMed: 29129651]
171. He J, Ogawa Y, Mukai S, et al. In Vivo Confocal Microscopy Evaluation of Ocular Surface with Graft-Versus-Host Disease-Related Dry Eye Disease. Sci Rep. 2017;7(1):10720. [PubMed: 28878217]
172. Long Q, Zuo YG, Yang X, Gao TT, Liu J, Li Y. Clinical features and in vivo confocal microscopy assessment in 12 patients with ocular cicatricial pemphigoid. Int J Ophthalmol. 2016;9(5):730–737. [PubMed: 27275431]
173. Mantopoulos D, Cruzat A, Hamrah P. In vivo imaging of corneal inflammation: new tools for clinical practice and research. Semin Ophthalmol. 2010;25(5-6):178–185. [PubMed: 21090997]
174. Villani E, Galimberti D, Del Papa N, Nucci P, Ratiglia R. Inflammation in dry eye associated with rheumatoid arthritis: cytokine and in vivo confocal microscopy study. Innate Immun. 2013;19(4):420–427. [PubMed: 23339928]
175. Pahuja NK, Shetty R, Deshmukh R, et al. In vivo confocal microscopy and tear cytokine analysis in post-LASIK ectasia. Br J Ophthalmol. 2017;101(12):1604–1610. [PubMed: 28450380]
176. Hillenaar T, van Cleynenbreugel H, Verjans GM, Wubbels RJ, Remeijer L. Monitoring the inflammatory process in herpetic stromal keratitis: the role of in vivo confocal microscopy. Ophthalmology. 2012;119(6):1102–1110. [PubMed: 22361312]
177. Semeraro F, Forbice E, Nascimbeni G, et al. Effect of Autologous Serum Eye Drops in Patients with Sjogren Syndrome-related Dry Eye: Clinical and In Vivo Confocal Microscopy Evaluation of the Ocular Surface. In Vivo. 2016;30(6):931–938. [PubMed: 27815483]
178. Randon M, Liang H, Abbas R, et al. [A new classification for meibomian gland diseases with in vivo confocal microscopy]. J Fr Ophtalmol. 2016;39(3):239–247. [PubMed: 26896195]
179. Oliveira-Soto L, Efron N. Morphology of corneal nerves using confocal microscopy. Cornea. 2001;20(4):374–384. [PubMed: 11333324]
180. Guthoff RF, Wienss H, Hahnel C, Wree A. Epithelial innervation of human cornea: a three-dimensional study using confocal laser scanning fluorescence microscopy. Cornea. 2005;24(5):608–613. [PubMed: 15968170]
181. Patel DV, Tavakoli M, Craig JP, Efron N, McGhee CN. Corneal sensitivity and slit scanning in vivo confocal microscopy of the subbasal nerve plexus of the normal central and peripheral human cornea. Cornea. 2009;28(7):735–740. [PubMed: 19574916]
182. Petropoulos IN, Manzoor T, Morgan P, et al. Repeatability of in vivo corneal confocal microscopy to quantify corneal nerve morphology. Cornea. 2013;32(5):e83–89. [PubMed: 23172119]
183. Pacaud D, Romanchuk KG, Tavakoli M, et al. The Reliability and Reproducibility of Corneal Confocal Microscopy in Children. Invest Ophthalmol Vis Sci. 2015;56(9):5636–5640. [PubMed: 26313299]
184. Hamrah P, Qazi Y, Shahatit B, et al. Corneal Nerve and Epithelial Cell Alterations in Corneal Allodynia: An In Vivo Confocal Microscopy Case Series. Ocul Surf. 2017;15(1):139–151. [PubMed: 27816571]
185. Cruzat A, Qazi Y, Hamrah P. In Vivo Confocal Microscopy of Corneal Nerves in Health and Disease. Ocul Surf. 2017;15(1):15–47. [PubMed: 27771327]
186. Brines M, Culver DA, Ferdousi M, et al. Corneal nerve fiber size adds utility to the diagnosis and assessment of therapeutic response in patients with small fiber neuropathy. Sci Rep. 2018;8(1):4734. [PubMed: 29549285]

187. Patel DV, McGhee CN. In vivo confocal microscopy of human corneal nerves in health, in ocular and systemic disease, and following corneal surgery: a review. Br J Ophthalmol. 2009;93(7):853–860. [PubMed: 19019923]

188. Erie JC, McLaren JW, Patel SV. Confocal microscopy in ophthalmology. Am J Ophthalmol. 2009;148(5):639–646. [PubMed: 19674730]

189. Hertz P, Bril V, Orszag A, et al. Reproducibility of in vivo corneal confocal microscopy as a novel screening test for early diabetic sensorimotor polyneuropathy. Diabet Med. 2011;28(10):1253–1260. [PubMed: 21434993]

190. Midena E, Cortese M, Miotto S, Gambato C, Cavarzeran F, Ghirlando A. Confocal microscopy of corneal sub-basal nerve plexus: a quantitative and qualitative analysis in healthy and pathologic eyes. J Refract Surg. 2009;25(1 Suppl):S125–130. [PubMed: 19248541]

191. Kalteniece A, Ferdousi M, Adam S, et al. Corneal confocal microscopy is a rapid reproducible ophthalmic technique for quantifying corneal nerve abnormalities. PLoS One. 2017;12(8):e0183040. [PubMed: 28817609]

192. Parissi M, Karanis G, Randjelovic S, et al. Standardized baseline human corneal subbasal nerve density for clinical investigations with laser-scanning in vivo confocal microscopy. Invest Ophthalmol Vis Sci. 2013;54(10):7091–7102. [PubMed: 24084094]

193. Wu T, Ahmed A, Bril V, et al. Variables associated with corneal confocal microscopy parameters in healthy volunteers: implications for diabetic neuropathy screening. Diabet Med. 2012;29(9):e297–303. [PubMed: 22519850]

194. Kim G, Singleton JR, Mifflin MD, Digre KB, Porzio MT, Smith AG. Assessing the Reproducibility of Quantitative In Vivo Confocal Microscopy of Corneal Nerves in Different Corneal Locations. Cornea. 2013;32(10):1331–1338. [PubMed: 23974884]

195. Benitez del Castillo JM, Wasfy MA, Fernandez C, Garcia-Sanchez J. An in vivo confocal masked study on corneal epithelium and subbasal nerves in patients with dry eye. Invest Ophthalmol Vis Sci. 2004;45(9):3030–3035. [PubMed: 15326117]

196. Zhang M, Chen J, Luo L, Xiao Q, Sun M, Liu Z. Altered corneal nerves in aqueous tear deficiency viewed by in vivo confocal microscopy. Cornea. 2005;24(7):818–824. [PubMed: 16160498]

197. Grupcheva CN, Wong T, Riley AF, McGhee CN. Assessing the sub-basal nerve plexus of the living healthy human cornea by in vivo confocal microscopy. Clin Exp Ophthalmol. 2002;30(3):187–190. [PubMed: 12010212]

198. Hosal BM, Ornek N, Zilelioglu G, Elhan AH. Morphology of corneal nerves and corneal sensation in dry eye: a preliminary study. Eye (Lond). 2005;19(12):1276–1279. [PubMed: 15550934]

199. Nubile M, Mastropasqua L. In vivo confocal microscopy of the ocular surface: where are we now? Br J Ophthalmol. 2009;93(7):850–852. [PubMed: 19553510]

200. Aggarwal S, Kheirkhah A, Cavalcanti BM, et al. Autologous Serum Tears for Treatment of Photoallodynia in Patients with Corneal Neuropathy: Efficacy and Evaluation with In Vivo Confocal Microscopy. Ocul Surf. 2015;13(3):250–262. [PubMed: 26045233]

201. Aggarwal S, Colon C, Kheirkhah A, Hamrah P. Efficacy of autologous serum tears for treatment of neuropathic corneal pain. Ocul Surf. 2019.

202. Giannaccare G, Buzzi M, Fresina M, Velati C, Versura P. Efficacy of 2-Month Treatment With Cord Blood Serum Eye Drops in Ocular Surface Disease: An In Vivo Confocal Microscopy Study. Cornea. 2017;36(8):915–921. [PubMed: 28679130]

203. Hamrah P, Cruzat A, Dastjerdi MH, et al. Corneal sensation and subbasal nerve alterations in patients with herpes simplex keratitis: an in vivo confocal microscopy study. Ophthalmology. 2010;117(10):1930–1936. [PubMed: 20810171]

204. Nagasato D, Araki-Sasaki K, Kojima T, Ideta R, Dogru M. Morphological changes of corneal subepithelial nerve plexus in different types of herpetic keratitis. Jpn J Ophthalmol. 2011;55(5):444–450. [PubMed: 21830060]

205. Moein HR, Kheirkhah A, Muller RT, Cruzat AC, Pavan-Langston D, Hamrah P. Corneal nerve regeneration after herpes simplex keratitis: A longitudinal in vivo confocal microscopy study. Ocul Surf. 2018;16(2):218–225. [PubMed: 29305292]

206. Hamrah P, Cruzat A, Dastjerdi MH, et al. Unilateral herpes zoster ophthalmicus results in bilateral corneal nerve alteration: an in vivo confocal microscopy study. Ophthalmology. 2013;120(1):40–47. [PubMed: 22999636]

207. Sacchetti M, Lambiase A. Diagnosis and management of neurotrophic keratitis. Clin Ophthalmol. 2014;8:571–579. [PubMed: 24672223]

208. Parissi M, Randjelovic S, Poletti E, et al. Corneal Nerve Regeneration After Collagen Cross-Linking Treatment of Keratoconus: A 5-Year Longitudinal Study. JAMA Ophthalmol. 2016;134(1):70–78. [PubMed: 26562763]

209. Leonardi A, Lazzarini D, Bortolotti M, Piliego F, Midena E, Fregona I. Corneal confocal microscopy in patients with vernal keratoconjunctivitis. Ophthalmology. 2012;119(3):509–515. [PubMed: 22176802]

210. Hu Y, Matsumoto Y, Adan ES, et al. Corneal in vivo confocal scanning laser microscopy in patients with atopic keratoconjunctivitis. Ophthalmology. 2008;115(11):2004–2012. [PubMed: 18584874]

211. Deng SX, Sejpal KD, Tang Q, Aldave AJ, Lee OL, Yu F. Characterization of limbal stem cell deficiency by in vivo laser scanning confocal microscopy: a microstructural approach. Archives of ophthalmology. 2012;130(4):440–445. [PubMed: 22159172]

212. Chuephanich P, Supiyaphun C, Aravena C, Bozkurt TK, Yu F, Deng SX. Characterization of the Corneal Subbasal Nerve Plexus in Limbal Stem Cell Deficiency. Cornea. 2017;36(3):347–352. [PubMed: 27941384]

213. Deak EA, Szalai E, Toth N, Malik RA, Berta A, Csutak A. Longitudinal Changes in Corneal Cell and Nerve Fiber Morphology in Young Patients with Type 1 Diabetes with and without Diabetic Retinopathy: A 2-Year Follow-up Study. Invest Ophthalmol Vis Sci. 2019;60(2):830–837. [PubMed: 30811546]

214. dell'Omo R, Cifariello F, De Turris S, et al. Confocal microscopy of corneal nerve plexus as an early marker of eye involvement in patients with type 2 diabetes. Diabetes Res Clin Pract. 2018;142:393–400. [PubMed: 29935212]

215. Villani E, Viola F, Sala R, et al. Corneal involvement in Graves' orbitopathy: an in vivo confocal study. Invest Ophthalmol Vis Sci. 2010;51(9):4574–4578. [PubMed: 20435595]

216. Mikolajczak J, Zimmermann H, Kheirkhah A, et al. Patients with multiple sclerosis demonstrate reduced subbasal corneal nerve fibre density. Mult Scler. 2017;23(14):1847–1853. [PubMed: 27811337]

217. Petropoulos IN, Kamran S, Li Y, et al. Corneal Confocal Microscopy: An Imaging Endpoint for Axonal Degeneration in Multiple Sclerosis. Invest Ophthalmol Vis Sci. 2017;58(9):3677–3681. [PubMed: 28727882]

218. Misra SL, Kersten HM, Roxburgh RH, Danesh-Meyer HV, McGhee CN. Corneal nerve microstructure in Parkinson's disease. J Clin Neurosci. 2017;39:53–58. [PubMed: 28268149]

219. Bucher F, Schneider C, Blau T, et al. Small-Fiber Neuropathy Is Associated With Corneal Nerve and Dendritic Cell Alterations: An In Vivo Confocal Microscopy Study. Cornea. 2015;34(9):1114–1119. [PubMed: 26186372]

220. Cardigos J, Barcelos F, Carvalho H, et al. Tear Meniscus and Corneal Sub-basal Nerve Plexus Assessment in Primary Sjogren Syndrome and Sicca Syndrome Patients. Cornea. 2019;38(2):221–228. [PubMed: 30379721]

221. Benitez-Del-Castillo JM, Acosta MC, Wassfi MA, et al. Relation between corneal innervation with confocal microscopy and corneal sensitivity with noncontact esthesiometry in patients with dry eye. Invest Ophthalmol Vis Sci. 2007;48(1):173–181. [PubMed: 17197530]

222. Labbe A, Alalwani H, Van Went C, Brasnu E, Georgescu D, Baudouin C. The relationship between subbasal nerve morphology and corneal sensation in ocular surface disease. Invest Ophthalmol Vis Sci. 2012;53(8):4926–4931. [PubMed: 22695962]

223. Villani E, Galimberti D, Viola F, Mapelli C, Ratiglia R. The cornea in Sjogren's syndrome: an in vivo confocal study. Invest Ophthalmol Vis Sci. 2007;48(5):2017–2022. [PubMed: 17460255]

224. Labbe A, Liang Q, Wang Z, et al. Corneal nerve structure and function in patients with non-sjogren dry eye: clinical correlations. Invest Ophthalmol Vis Sci. 2013;54(8):5144–5150. [PubMed: 23833066]

225. Iaccheri B, Torroni G, Cagini C, et al. Corneal confocal scanning laser microscopy in patients with dry eye disease treated with topical cyclosporine. Eye (Lond). 2017;31(5):788–794. [PubMed: 28157225]

226. Levy O, Labbe A, Borderie V, et al. Increased corneal sub-basal nerve density in patients with Sjogren syndrome treated with topical cyclosporine A. Clin Exp Ophthalmol. 2017;45(5):455–463. [PubMed: 27957797]

227. Zemaitiene R, Rakauskiene M, Danileviciene V, Use V, Kriauciuniene L, Zaliuniene D. Corneal esthesiometry and sub-basal nerves morphological changes in herpes simplex virus keratitis/uveitis patients. Int J Ophthalmol. 2019;12(3):407–411. [PubMed: 30918808]

228. Muller RT, Pourmirzaie R, Pavan-Langston D, et al. In Vivo Confocal Microscopy Demonstrates Bilateral Loss of Endothelial Cells in Unilateral Herpes Simplex Keratitis. Invest Ophthalmol Vis Sci. 2015;56(8):4899–4906. [PubMed: 26225629]

229. Lambiase A, Sacchetti M, Mastropasqua A, Bonini S. Corneal changes in neurosurgically induced neurotrophic keratitis. JAMA Ophthalmol. 2013;131(12):1547–1553. [PubMed: 24158681]

230. John T, Tighe S, Sheha H, et al. Corneal Nerve Regeneration after Self-Retained Cryopreserved Amniotic Membrane in Dry Eye Disease. J Ophthalmol. 2017;2017:6404918. [PubMed: 28894606]

231. Fung SSM, Catapano J, Elbaz U, Zuker RM, Borschel GH, Ali A. In Vivo Confocal Microscopy Reveals Corneal Reinnervation After Treatment of Neurotrophic Keratopathy With Corneal Neurotization. Cornea. 2018;37(1):109–112. [PubMed: 29053558]

232. Postorino EI, Rania L, Aragona E, et al. Efficacy of eyedrops containing cross-linked hyaluronic acid and coenzyme Q10 in treating patients with mild to moderate dry eye. Eur J Ophthalmol. 2018;28(1):25–31. [PubMed: 28777385]

233. Kallinikos P, Berhanu M, O'Donnell C, Boulton AJ, Efron N, Malik RA. Corneal nerve tortuosity in diabetic patients with neuropathy. Invest Ophthalmol Vis Sci. 2004;45(2):418–422. [PubMed: 14744880]

234. Rosenberg ME, Tervo TM, Immonen IJ, Muller LJ, Gronhagen-Riska C, Vesaluoma MH. Corneal structure and sensitivity in type 1 diabetes mellitus. Invest Ophthalmol Vis Sci. 2000;41(10):2915–2921. [PubMed: 10967045]

235. Midena E, Brugin E, Ghirlando A, Sommavilla M, Avogaro A. Corneal diabetic neuropathy: a confocal microscopy study. J Refract Surg. 2006;22(9 Suppl):S1047–1052. [PubMed: 17444092]

236. Edwards K, Pritchard N, Vagenas D, Russell A, Malik RA, Efron N. Utility of corneal confocal microscopy for assessing mild diabetic neuropathy: baseline findings of the LANDMark study. Clin Exp Optom. 2012;95(3):348–354. [PubMed: 22540156]

237. Tavakoli M, Quattrini C, Abbott C, et al. Corneal confocal microscopy: a novel noninvasive test to diagnose and stratify the severity of human diabetic neuropathy. Diabetes Care. 2010;33(8):1792–1797. [PubMed: 20435796]

238. Misra SL, Craig JP, Patel DV, et al. In Vivo Confocal Microscopy of Corneal Nerves: An Ocular Biomarker for Peripheral and Cardiac Autonomic Neuropathy in Type 1 Diabetes Mellitus. Invest Ophthalmol Vis Sci. 2015;56(9):5060–5065. [PubMed: 26241393]

239. Chang PY, Carrel H, Huang JS, et al. Decreased density of corneal basal epithelium and subbasal corneal nerve bundle changes in patients with diabetic retinopathy. Am J Ophthalmol. 2006;142(3):488–490. [PubMed: 16935596]

240. Messmer EM, Schmid-Tannwald C, Zapp D, Kampik A. In vivo confocal microscopy of corneal small fiber damage in diabetes mellitus. Graefes Arch Clin Exp Ophthalmol. 2010;248(9):1307–1312. [PubMed: 20490534]

241. Nitoda E, Kallinikos P, Pallikaris A, et al. Correlation of diabetic retinopathy and corneal neuropathy using confocal microscopy. Curr Eye Res. 2012;37(10):898–906. [PubMed: 22632054]

242. Zhivov A, Winter K, Hovakimyan M, et al. Imaging and quantification of subbasal nerve plexus in healthy volunteers and diabetic patients with or without retinopathy. PLoS One. 2013;8(1):e52157. [PubMed: 23341892]

243. Petropoulos IN, Green P, Chan AW, et al. Corneal confocal microscopy detects neuropathy in patients with type 1 diabetes without retinopathy or microalbuminuria. PLoS One. 2015;10(4):e0123517. [PubMed: 25853247]

244. Yan A, Issar T, Tummanapalli SS, et al. Relationship between corneal confocal microscopy and markers of peripheral nerve structure and function in Type 2 diabetes. Diabet Med. 2019.

245. Lagali NS, Allgeier S, Guimaraes P, et al. Reduced Corneal Nerve Fiber Density in Type 2 Diabetes by Wide-Area Mosaic Analysis. Invest Ophthalmol Vis Sci. 2017;58(14):6318–6327. [PubMed: 29242906]

246. Dehghani C, Pritchard N, Edwards K, Russell AW, Malik RA, Efron N. Abnormal Anterior Corneal Morphology in Diabetes Observed Using In Vivo Laser-scanning Confocal Microscopy. Ocul Surf. 2016;14(4):507–514. [PubMed: 27555566]

247. Jia X, Wang X, Wang X, et al. In Vivo Corneal Confocal Microscopy Detects Improvement of Corneal Nerve Parameters following Glycemic Control in Patients with Type 2 Diabetes. J Diabetes Res. 2018;2018:8516276. [PubMed: 30035129]

248. Tuominen IS, Konttinen YT, Vesaluoma MH, Moilanen JA, Helinto M, Tervo TM. Corneal innervation and morphology in primary Sjogren's syndrome. Invest Ophthalmol Vis Sci. 2003;44(6):2545–2549. [PubMed: 12766055]

249. Zhang X, Chen Q, Chen W, Cui L, Ma H, Lu F. Tear dynamics and corneal confocal microscopy of subjects with mild self-reported office dry eye. Ophthalmology. 2011;118(5):902–907. [PubMed: 21146227]

250. Annunziata R, Kheirkhah A, Aggarwal S, Hamrah P, Trucco E. A fully automated tortuosity quantification system with application to corneal nerve fibres in confocal microscopy images. Med Image Anal. 2016;32:216–232. [PubMed: 27136674]

251. Dieckmann G, Goyal S, Hamrah P. Neuropathic Corneal Pain: Approaches for Management. Ophthalmology. 2017;124(11s):S34–s47. [PubMed: 29055360]

252. Moein HRD G; Abbouda A; Pondelis N; Jamali A; Salem Z; Hamrah P In Vivo Confocal Microscopy Demonstrates the Presence of Microneuromas and may Allow Differentiation of Patients with Corneal Neuropathic Pain from Dry Eye Disease. Annual Meeting Abstract presented at The Association for Research in Vision and Ophthalomology; 2017; Baltimore, MA.

253. Kehlet H, Jensen TS, Woolf CJ. Persistent postsurgical pain: risk factors and prevention. Lancet. 2006;367(9522):1618–1625. [PubMed: 16698416]

254. Akhlaq AD, A.; Koseoglu ND; Kataguiri P; Hamrah P Subcategories of Neuropathic Corneal Pain: Epidemiology and Risk Factors. American Academy of Ophthalmology; 2018; Chicago, IL.

255. Li Y, Shekhar R, Huang D. Corneal pachymetry mapping with high-speed optical coherence tomography. Ophthalmology. 2006;113(5):792–799 e792. [PubMed: 16650675]

256. Li Y, Tan O, Brass R, Weiss JL, Huang D. Corneal epithelial thickness mapping by Fourier-domain optical coherence tomography in normal and keratoconic eyes. Ophthalmology. 2012;119(12):2425–2433. [PubMed: 22917888]

257. Rocha KM, Perez-Straziota CE, Stulting RD, Randleman JB. SD-OCT analysis of regional epithelial thickness profiles in keratoconus, postoperative corneal ectasia, and normal eyes. J Refract Surg. 2013;29(3):173–179. [PubMed: 23446013]

258. Temstet C, Sandali O, Bouheraoua N, et al. Corneal epithelial thickness mapping using Fourier-domain optical coherence tomography for detection of form fruste keratoconus. J Cataract Refract Surg. 2015;41(4):812–820. [PubMed: 25840306]

259. Kanellopoulos AJ, Asimellis G. OCT corneal epithelial topographic asymmetry as a sensitive diagnostic tool for early and advancing keratoconus. Clin Ophthalmol. 2014;8:2277–2287. [PubMed: 25429197]

260. Vega-Estrada A, Mimouni M, Espla E, Alio Del Barrio J, Alio JL. Corneal Epithelial Thickness Intrasubject Repeatability and its Relation With Visual Limitation in Keratoconus. Am J Ophthalmol. 2019;200:255–262. [PubMed: 30689987]

261. Reinstein DZ, Yap TE, Archer TJ, Gobbe M, Silverman RH. Comparison of Corneal Epithelial Thickness Measurement Between Fourier-Domain OCT and Very High-Frequency Digital Ultrasound. J Refract Surg. 2015;31(7):438–445. [PubMed: 26186562]

262. Ma XJ, Wang L, Koch DD. Repeatability of corneal epithelial thickness measurements using Fourier-domain optical coherence tomography in normal and post-LASIK eyes. Cornea. 2013;32(12):1544–1548. [PubMed: 24145634]
263. Sella R, Zangwill LM, Weinreb RN, Afshari NA. Repeatability and Reproducibility of Corneal Epithelial Thickness Mapping With Spectral-Domain Optical Coherence Tomography in Normal and Diseased Cornea Eyes. Am J Ophthalmol. 2019;197:88–97. [PubMed: 30240724]
264. Reinstein DZ, Srivannaboon S, Gobbe M, et al. Epithelial thickness profile changes induced by myopic LASIK as measured by Artemis very high-frequency digital ultrasound. J Refract Surg. 2009;25(5):444–450. [PubMed: 19507797]
265. Li Y, Chamberlain W, Tan O, Brass R, Weiss JL, Huang D. Subclinical keratoconus detection by pattern analysis of corneal and epithelial thickness maps with optical coherence tomography. J Cataract Refract Surg. 2016;42(2):284–295. [PubMed: 27026454]
266. Catalan S, Cadarso L, Esteves F, Salgado-Borges J, Lopez M, Cadarso C. Assessment of Corneal Epithelial Thickness in Asymmetric Keratoconic Eyes and Normal Eyes Using Fourier Domain Optical Coherence Tomography. J Ophthalmol. 2016;2016:5697343. [PubMed: 27379181]
267. Francoz M, Karamoko I, Baudouin C, Labbe A. Ocular surface epithelial thickness evaluation with spectral-domain optical coherence tomography. Invest Ophthalmol Vis Sci. 2011;52(12):9116–9123. [PubMed: 22025572]
268. Kanellopoulos AJ, Asimellis G. In vivo 3-dimensional corneal epithelial thickness mapping as an indicator of dry eye: preliminary clinical assessment. Am J Ophthalmol. 2014;157(1):63–68 e62. [PubMed: 24200234]
269. Le Q, Chen Y, Yang Y, Xu J. Measurement of corneal and limbal epithelial thickness by anterior segment optical coherence tomography and in vivo confocal microscopy. BMC Ophthalmol. 2016;16(1):163. [PubMed: 27645227]
270. Mehtani A, Agarwal MC, Sharma S, Chaudhary S. Diagnosis of limbal stem cell deficiency based on corneal epithelial thickness measured on anterior segment optical coherence tomography. Indian J Ophthalmol. 2017;65(11):1120–1126. [PubMed: 29133636]
271. Banayan N, Georgeon C, Grieve K, Borderie VM. Spectral-domain Optical Coherence Tomography in Limbal Stem Cell Deficiency. A Case-Control Study. Am J Ophthalmol. 2018;190:179–190. [PubMed: 29621511]
272. Chidambaram JD, Prajna NV, Palepu S, et al. In Vivo Confocal Microscopy Cellular Features of Host and Organism in Bacterial, Fungal, and Acanthamoeba Keratitis. Am J Ophthalmol. 2018;190:24–33. [PubMed: 29550185]
273. Gao YY, Di Pascuale MA, Li W, et al. High prevalence of Demodex in eyelashes with cylindrical dandruff. Invest Ophthalmol Vis Sci. 2005;46(9):3089–3094. [PubMed: 16123406]
274. Randon M, Liang H, El Hamdaoui M, et al. In vivo confocal microscopy as a novel and reliable tool for the diagnosis of Demodex eyelid infestation. Br J Ophthalmol. 2015;99(3):336–341. [PubMed: 25253768]
275. Liang H, Randon M, Michee S, Tahiri R, Labbe A, Baudouin C. In vivo confocal microscopy evaluation of ocular and cutaneous alterations in patients with rosacea. Br J Ophthalmol. 2017;101(3):268–274. [PubMed: 27222243]
276. Wang YJ, Ke M, Chen XM. Prospective study of the diagnostic accuracy of the in vivo laser scanning confocal microscope for ocular demodicosis. Am J Ophthalmol. 2019.
277. Huang P, Tepelus T, Vickers LA, et al. Quantitative Analysis of Depth, Distribution, and Density of Cysts in Acanthamoeba Keratitis Using Confocal Microscopy. Cornea. 2017;36(8):927–932. [PubMed: 28542085]
278. Goh JWY, Harrison R, Hau S, Alexander CL, Tole DM, Avadhanam VS. Comparison of In Vivo Confocal Microscopy, PCR and Culture of Corneal Scrapes in the Diagnosis of Acanthamoeba Keratitis. Cornea. 2018;37(4):480–485. [PubMed: 29256983]
279. Chidambaram JD, Prajna NV, Larke NL, et al. Prospective Study of the Diagnostic Accuracy of the In Vivo Laser Scanning Confocal Microscope for Severe Microbial Keratitis. Ophthalmology. 2016;123(11):2285–2293. [PubMed: 27538797]

280. Kheirkhah A, Satitpitakul V, Syed ZA, et al. Factors Influencing the Diagnostic Accuracy of Laser-Scanning In Vivo Confocal Microscopy for Acanthamoeba Keratitis. Cornea. 2018;37(7):818–823. [PubMed: 29303889]

281. Kanavi MR, Javadi M, Yazdani S, Mirdehghanm S. Sensitivity and specificity of confocal scan in the diagnosis of infectious keratitis. Cornea. 2007;26(7):782–786. [PubMed: 17667609]

282. Kheirkhah A, Syed ZA, Satitpitakul V, et al. Sensitivity and Specificity of Laser-Scanning In Vivo Confocal Microscopy for Filamentous Fungal Keratitis: Role of Observer Experience. Am J Ophthalmol. 2017;179:81–89. [PubMed: 28445703]

283. Chidambaram JD, Prajna NV, Larke N, et al. In vivo confocal microscopy appearance of Fusarium and Aspergillus species in fungal keratitis. Br J Ophthalmol. 2017;101(8):1119–1123. [PubMed: 28043985]

284. Daas L, Viestenz A, Schnabel PA, et al. Confocal microscopy as an early relapse marker for acanthamoeba keratitis. Clin Anat. 2018;31(1):60–63. [PubMed: 28556202]

285. Wang YE, Tepelus TC, Gui W, Irvine JA, Lee OL, Hsu HY. Reduction of Acanthamoeba Cyst Density Associated With Treatment Detected by In Vivo Confocal Microscopy in Acanthamoeba Keratitis. Cornea. 2019;38(4):463–468. [PubMed: 30640249]

286. Ting DSW, Pasquale LR, Peng L, et al. Artificial intelligence and deep learning in ophthalmology. Br J Ophthalmol. 2018.

287. Koseoglu NDB A; Hamrah P The Utilization of Artificial Intelligence for Corneal Nerve Analyses of In Vivo Confocal Microscopy Images for the Diagnosis of Neuropathic Corneal Pain. ARVO Annual Meeting; 2018; New Orleans, LA.

288. Cai Y, Alio Del Barrio JL, Wilkins MR, Ang M. Serial optical coherence tomography angiography for corneal vascularization. Graefes Arch Clin Exp Ophthalmol. 2017;255(1):135–139. [PubMed: 27722920]

289. Brunner M, Romano V, Steger B, et al. Imaging of Corneal Neovascularization: Optical Coherence Tomography Angiography and Fluorescence Angiography. Invest Ophthalmol Vis Sci. 2018;59(3):1263–1269. [PubMed: 29625447]

290. Binotti WN R; Dieckmann G; Kenyon K; Hamrah P Limbal Vascular Changes in Limbal Stem Cell Deficiency with Anterior Segment Optical Coherence Tomography Angiography. ARVO Annual Meeting; 2019; Vancouver, BC.

291. Binotti WN R; Mills H.; Wu H.; Hamrah P Anterior Segment Multimodal Optical Coherence Tomography Approach in the Assessment of Ocular Surface Neoplasia. American Academy of Ophthalmology; 2018; Chicago, IL.

292. Keech A, Flanagan J, Simpson T, Jones L. Tear meniscus height determination using the OCT2 and the RTVue-100. Optom Vis Sci. 2009;86(10):1154–1159. [PubMed: 19741561]

293. Savini G, Goto E, Carbonelli M, Barboni P, Huang D. Agreement between stratus and visante optical coherence tomography systems in tear meniscus measurements. Cornea. 2009;28(2):148–151. [PubMed: 19158555]

294. Akiyama R, Usui T, Yamagami S. Diagnosis of Dry Eye by Tear Meniscus Measurements Using Anterior Segment Swept Source Optical Coherence Tomography. Cornea. 2015;34 Suppl 11:S115–120. [PubMed: 26448168]

295. Schulze MM, Hutchings N, Simpson TL. The perceived bulbar redness of clinical grading scales. Optom Vis Sci. 2009;86(11):E1250–1258. [PubMed: 19770812]

296. Schulze MM, Hutchings N, Simpson TL. The conversion of bulbar redness grades using psychophysical scaling. Optom Vis Sci. 2010;87(3):159–167. [PubMed: 20125060]

297. Schulze MM, Hutchings N, Simpson TL. Grading bulbar redness using cross-calibrated clinical grading scales. Invest Ophthalmol Vis Sci. 2011;52(8):5812–5817. [PubMed: 21474775]

298. Wang Y, Zhao F, Zhu W, Xu J, Zheng T, Sun X. In vivo confocal microscopic evaluation of morphologic changes and dendritic cell distribution in pterygium. Am J Ophthalmol. 2010;150(5):650–655 e651. [PubMed: 20691419]

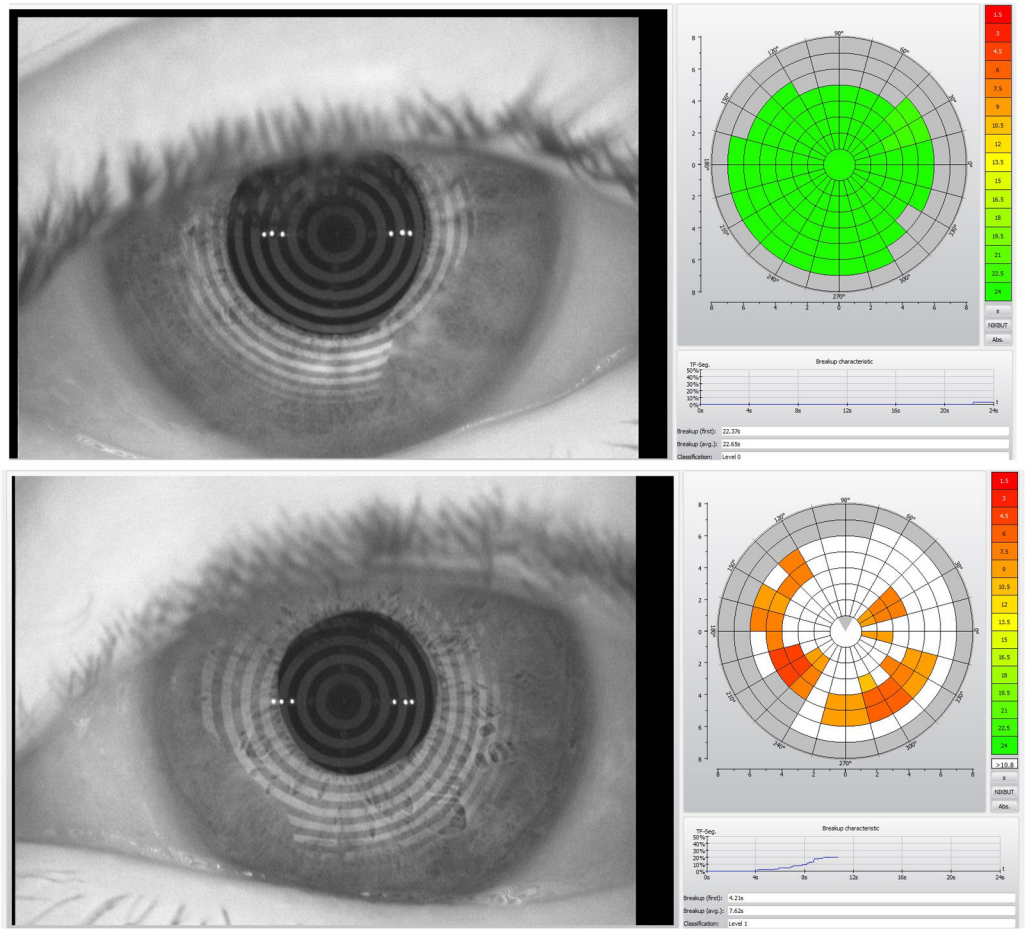

Figure 1.

Non-invasive tear film break-up time measurement by Oculus Keratograph 5M (Oculus, Arlington, WA, USA). **a**) Normal tear film break-up time with regular pattern. **b**) First and average break-up times were lower than normal values based on color scale in a patient with evaporative dry eye disease (movie of the same patient can be seen as supplementary data).

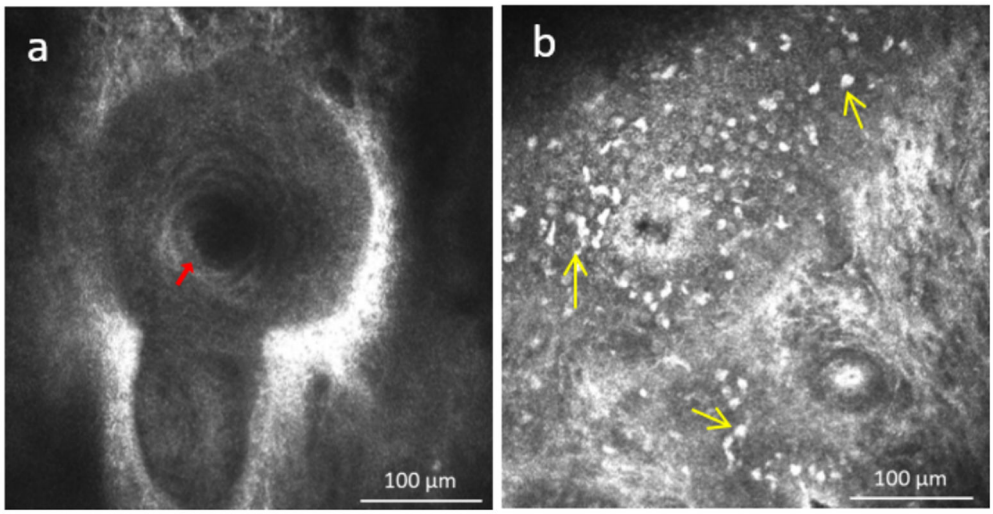

Figure 2.

a) In vivo confocal microscopy of the orifice of meibomian glands (red arrow) of the eyelid and **b)** presence of immune cells (yellow arrows) surrounding acinar unit.

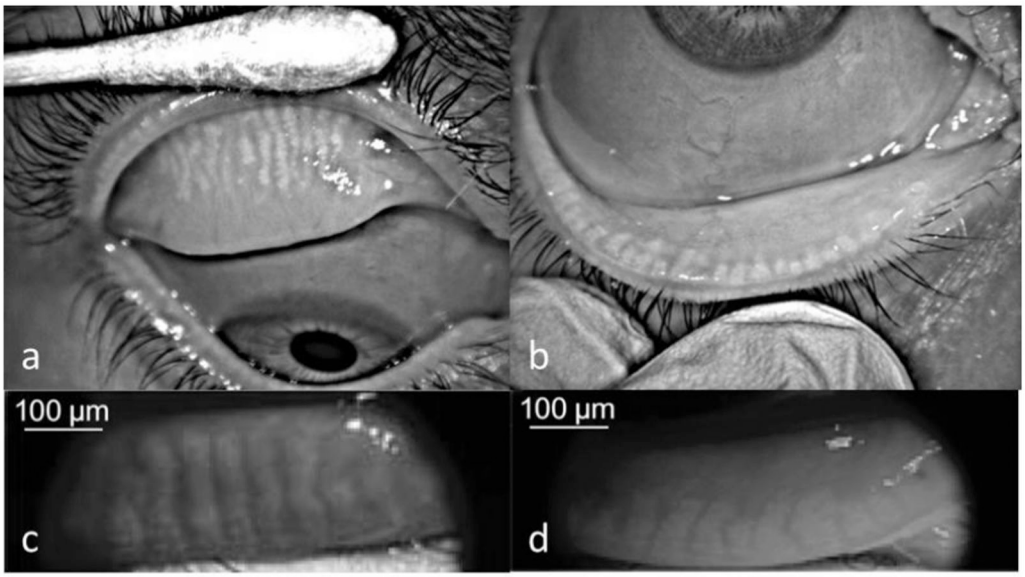

Figure 3.

Meibography images (Infrared 840 nm) recorded by Oculus Keratograph 5M (Oculus, Arlington, WA, USA) **a)** Meibomian glands with moderate dropout and increased tortuosity of the glands are seen on the upper eyelid. **b)** Lower eyelid: severe dropout and dilatation of meibomian glands can be seen. Meibography images (nearinfrared 735 nm) of **c)** upper and **d)** lower eyelid recorded by Optovue RTVue-XR Avanti OCT System (Optovue, Fremont, CA, USA)

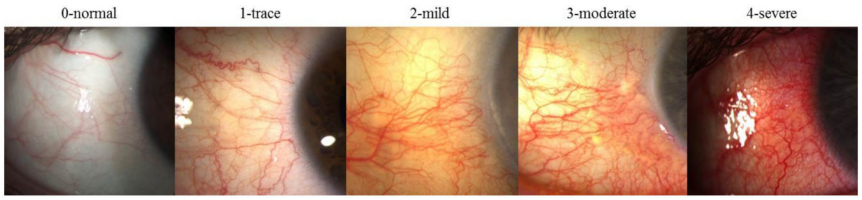

Figure 4.
Example of ocular redness grading scales and classification according to severity.

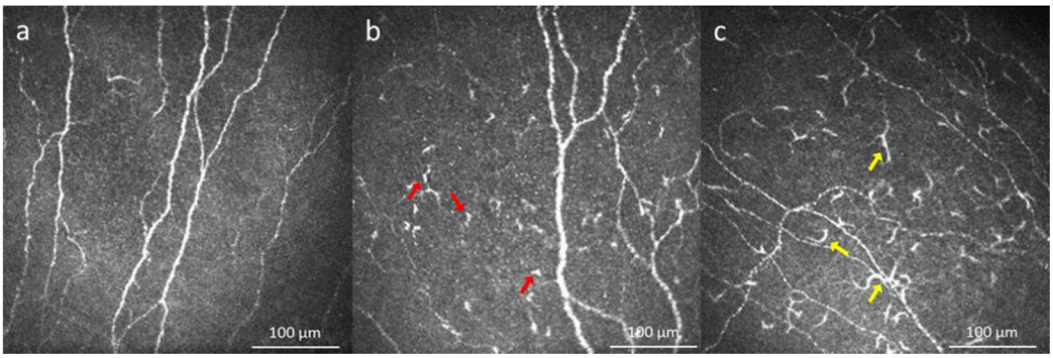

Figure 5.

In vivo confocal microscopy images in dry eye disease: **a)** Healthy individual. **b)** Increased number of dendritiform cells in patients with dry eye disease (red arrows show representative cells). c) Increased number of presumed mature dendritiform cells in patient with dry eye disease (yellow arrows show representative cells).

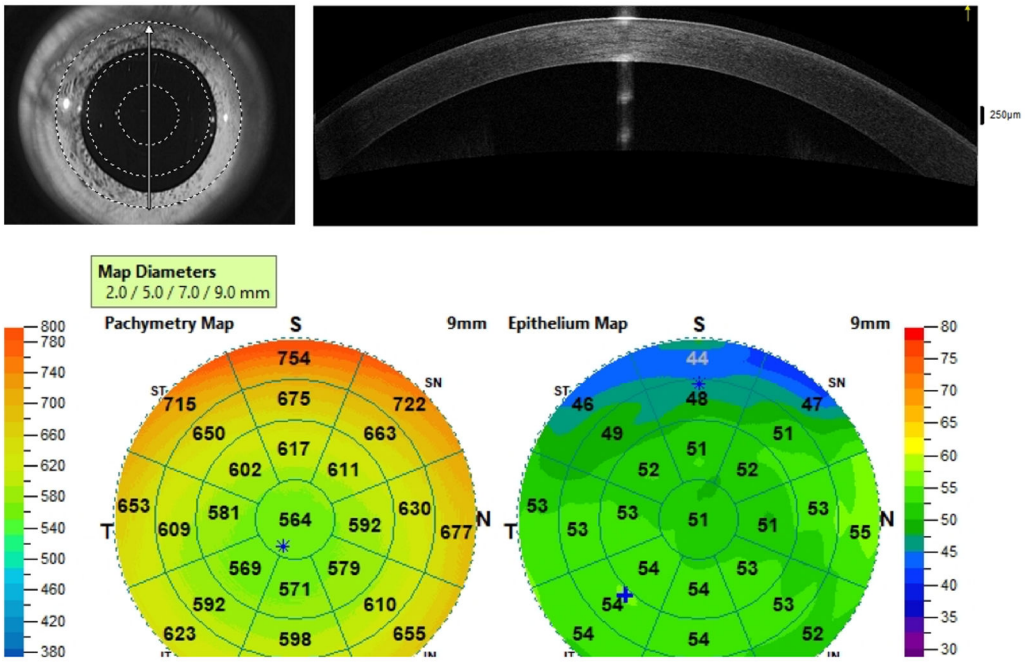

Figure 6.

Subbasal nerves detected by IVCM. **a)** Subbasal nerves in a normal indiviual; **b)** Decreased main nerve density (pink traces) and decreased nerve branching (blue tracing) in herpes simplex keratitis; **c)** Absence of subbasal nerve plexus in neurotrophic keratitis secondary to herpes simplex keratitis; **d)** Increased nerve tortuosity in dry eye disease (two semicircles on the same nerve branch shows most representative areas); **e)** Increased beading in a patient with neuropathic corneal pain (most representative beading areas are bordered by blue stars); **e, f)** Hyperreflective abnormal bulging of corneal nerve ending, microneuromas in patient with neuropathic corneal pain (green arrow heads).

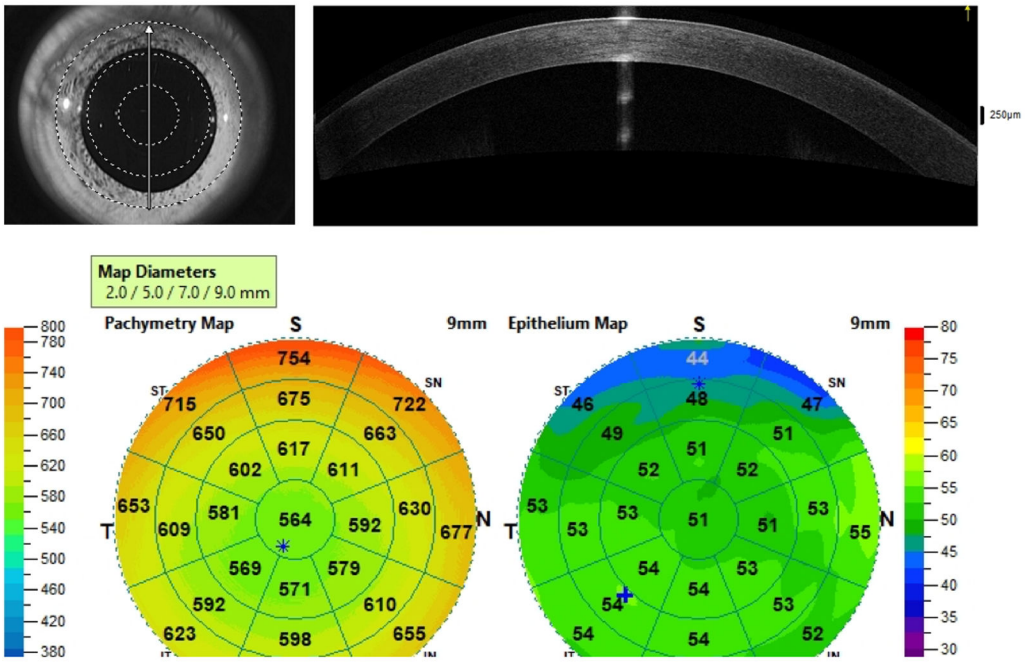

Figure 7.

Anterior segment Optical Coherence Tomography (AS-OCT) corneal thickness and corneal epithelial thickness maps in a healthy eye. **a)** Reference infrared image and direction of selected scan (arrow). **b)** AS-OCT line of the cornea. **c)** Pachymetry and epithelial thickness color-coded maps.

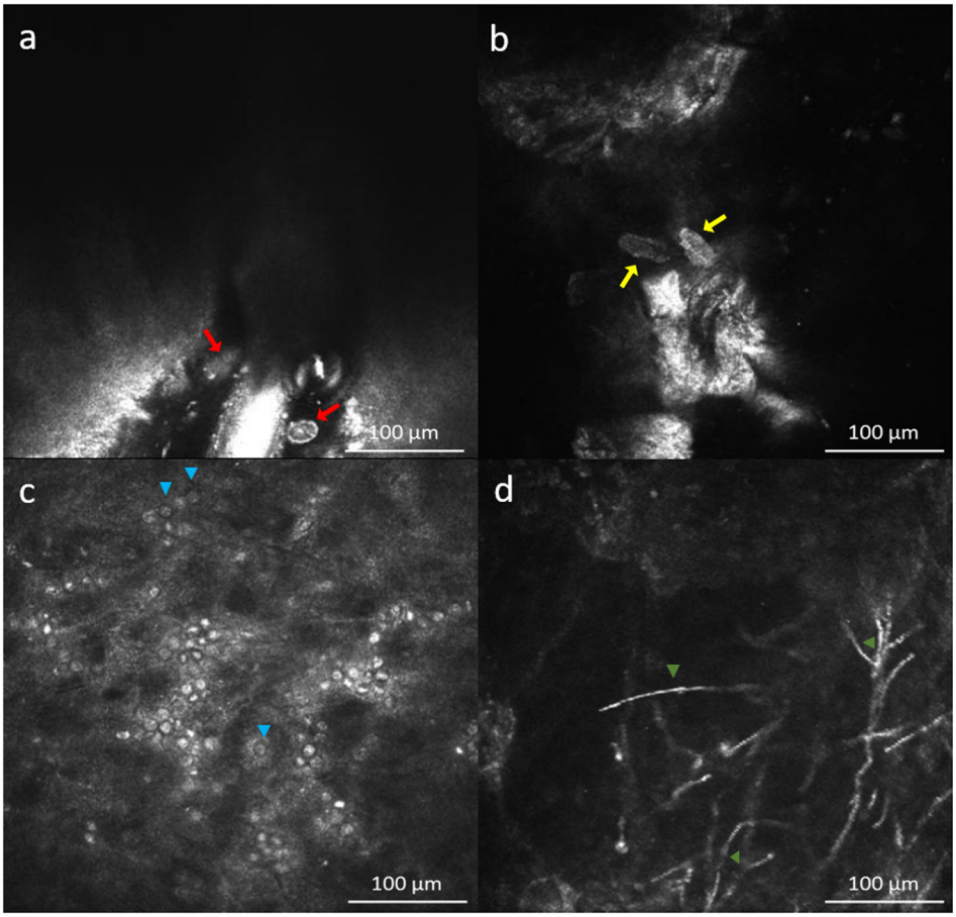

Figure 8.

In vivo confocal microscopy images in infectious keratitis. **a)** Ovoid hyperreflective structure at the base of eyelash follicle of Demodex follicularis (red arrows) and **b)** Demodex brevis (yellow arrows). **c)** Double walled cysts (blue arrow heads) with hyperreflective center and hyporeflective surrounding halo and hyperreflective ovoid trophozoites in *Acanthomoeba* keratitis; **d)** Hyperreflective septated thin filamentous structures at anterior stroma in filamentous fungal keratitis (orange arrow heads).

Table 1-

Validation Characteristics [1,6]

Analytical validation	**Demonstration of the accuracy, precision, and feasibility of biomarker measurement.**
• Accuracy	Closeness of agreement between the image acquired and the actual anatomical appearance
• Reference normal value	Normal distribution of values in a healthy population
• Precision	Closeness of agreement between a series of images obtained from multiple sampling of the same homogeneous sample under the prescribed conditions:
◦ Repeatability/Intra-grader reliability	The agreement between successive measurements made under the same conditions.
◦ Reproducibility/Inter-grader reliability	The agreement between successive measurements made with varying conditions, such as location or operator.

Table 2-

Biomarker Definitions[1,6]

Clinical validation	**A process to establish that the test, tool, or instrument acceptably identifies, measures, or predicts the concept, which is the aspect of an individual's clinical, biological, physical, or functional state, or experience that the assessment is intended to capture or reflect, of interest (the aspects necessary for clinical validation are dependent on the type of biomarker being developed)**
• Diagnostic biomarker	A biomarker used to detect or confirm presence of a disease or condition of interest or to identify individuals with a subtype of the disease
◦ Sensitivity	Measures the ability of a diagnostic biomarker to correctly classify the presence of a particular condition/disease in patients that have the condition/disease.
◦ Specificity	Measures the ability of a diagnostic biomarker to correctly classify the absence of a particular condition/disease in patients that do not have the condition/disease.
• Monitoring biomarker	A biomarker measured serially for assessing status of a disease or medical condition or for evidence of exposure to (or effect of) a medical product or an environmental agent
• Prognostic biomarker	A biomarker used to identify likelihood of a clinical event, disease recurrence or progression in patients who have the disease or medical condition of interest
• Predictive biomarker	A biomarker used to identify individuals who are more likely than similar individuals without the biomarker to experience a favorable or unfavorable effect from exposure to a medical product or an environmental agent
• Pharmacodynamic/ response biomarker	A biomarker used to show that a biological response has occurred in an individual who has been exposed to a medical product or an environmental agent
• Safety biomarker	A biomarker measured before or after an exposure to a medical product or an environmental agent to indicate the likelihood, presence, or extent of toxicity as an adverse effect
• Susceptibility/risk biomarker	A biomarker that indicates the potential for developing a disease or medical condition in an individual who does not currently have clinically apparent disease or the medical condition

Table 3.

Summary of the Biomarkers' Analytical and Clinical Validation.

		Analytical Validation		Clinical Validation			
Biomarkers	Normal Range	Repeatability/ Intra-observer reliability	Reproducibility/ Inter-observer reliability	Diagnostic		Monitoring	Predictive
				Sensitivity	Specificity		
NIBUT	≥10 seconds	CoV= 7.3-36.6%[18,26,27] ICC= 0.750-0.930[18,23,25-27]	CoV= 15.4-21.85%18,[27] ICC= 0.880[27]	80.0-87.0% [29-31]	86.0-100% [29-31]	✓	✓
TMH							
• Time Domain	230-332 μm[42,45,51]	CoV= 21.3-49.6%[42,51,292,293]	S_p= ±29μm[36,51]	67.0%[42]	81.0%[42]	✓	
• Spectral Domain	319-354 μm[36,51]	CoV= 9.0-28.4%[39,40,51,53] ICC= 0.900-0.981[39,40,51,53]	S_p= ±15μm[36,51] CoV= 7.0-17.1%[39,40,51,53] ICC= 0.920-0.930[39,40,51,53]	80.5%	89.3%	✓	
• Swept-Source	183-339 μm[39,40,51,53]	CoV= 23.9-28.0%[48,294] ICC= 0.909-0.981[48,294]	CoV= 14.5-28.0%[48,294] ICC= 0.932-0.948[48,294]	67.0%	88.0%	✓	
TMA							
• Time Domain	3,414-35,283 μm^2 [15,39,48-50]					✓	
• Spectral Domain	25,383-62,100 μm2 [15,39,48-50]	CoV = 17.0-44.0%[53,54,292]	CoV = 19.5-35.4%[53,54,292]	86.1%	85.3%	✓	
• Swept-Source	12,459-27,900 μm^2 [15,39,48-50]	CoV= 45.5-52.0%[48,294] ICC= 0.873-0.990[48,294]	CoV= 27.7-29.4%[48,294] ICC=0.813-0.982[48,294]	62.0%	92.0%	✓	

NIBUT: non-invasive tear break-up time, TMH: tear meniscus height, TMA: tear meaniscus area, Sp= pooled standard deviation, CoV: coefficient of variability, ICC: intra- or inter-class correlation coefficient.

Table 4.

Summary of the Biomarkers' Analytical and Clinical Validation.

		Analytical Validation		Clinical Validation			
Biomarkers	Normal Range	Repeatability/ Intra-observer reliability	Reproducibility/ Inter-observer reliability	Diagnostic		Monitoring	Predictive
				Sensitivity	Specificity		
IR Meibography				49-88%[48,292]	65-100%[48,292]		
• % parcial gland		k_w= 0.15 to 0.91[81]	K_w= 0.36-0.77[81,82]				
• % gland drop out		k_w= 0.40-0.81[82]	K_w= 0.21-0.90[82,85]			✓	
• software analysis		ICC= 0.570-0.740[82]	ICC= 0.520-0.870[85,93]			✓	
OR							
• Scales	0 grade [0-3/4]	CoV= 17-20%[100-102,104] CoR= 0.31-0.59[100-102,104] ICC= 0.980[100-102,104]	CoR= 0.49-0.80[100-102,104]			✓	✓
• VBR	-	CoV= 3.9-9.1%[107,295-297]	CoR= 5.0-5.9 ICC= 0.992-0.999[107,295-297]			✓	✓
• ORI	-	-	ICC= 0.995-0.998[108]			✓	✓
Dendritiform Cells	Central: 9-64 cells/mm^2 [130,158,159,298] Peripheral: 0-208 cells/mm^2 [130,158,159,298]	CoV= 4.4-11.9%[75,131-139]	ICC= 0.991-0.997[75,131-139]			✓	✓
Palpebral Inflammation						✓	
• Immune cells on IVCM	Epithelial: 123.3-123.7 cells/mm^2 [74,178] Stromal: 36.7-38.8 cells/mm^2 [74,178]	ICC= 0.960-0.970[74,75]	ICC= 0.920-0.997[74,75]	94.0%[75]	92.0%[75]	✓	
Nerve Length	17.1-31.7 mm/mm^2 [179,184,185,187-189]	ICC= 0.700-0.980[182,189] DM ICC=0.980[189]	ICC= 0.610-0.940[182,189]	DED: 81.9%[185]	DED: 85.0%[185]	✓	✓
Nerve Density	8.4-31.9 mm/ mm^2[179,184,185,187-189]	ICC= 0.670-0.920[182,189] DM ICC=0.840[189,189]	ICC= 0.520-0.960[182,189]	DM: 82.0%[239-242] DED: 80.2%[185]	DM: 52.0%[239-242] DED: 85.0%[185]	✓	✓
Nerve Beading	90-198 beads/mm[182,190,194]	ICC= 0.930[187,195,196]	ICC= 0.870[187,195,196]			✓	
Nerve Tortuosity	1.1 grade [0-4] [192]	ICC= 0.200-0.690 [179,193,194]	ICC= 0.600-0.930 [179,193,194]	51.9 - 58.8%[250]	81.1 - 84.7%[250]	✓	
Nerve Reflectivity	1.1-2.6 grade[187,196,197]					✓	
Nerve Thickness	0.52-4.68 μm[182,190,194]					✓	

Eye Contact Lens. Author manuscript; available in PMC 2021 March 01.

Epithelial Corneal Thickness	50.4-53.4 μm[182]	Central CoV= 1.7-2.4%$^{256\text{-}260}$ Peripheral CoV=1.8-3.2%$^{256\text{-}260}$ ICC= 0.957-0.990	Central CoV= 0.4-3.6%$^{256\text{-}260}$ Peripheral CoV=2.4-3.8%$^{256\text{-}260}$ ICC= 0.891-0.970	AUC= 0.640-0.880 AUCPSD= 0.985-1.000	✓	✓